2011

Telma Bernardo Dimethylaminopyridine Derivatives of Lupane Triterpenoids Acting as Mitochondrial-Directed Agents on Breast Cancer Cells

DEPARTAMENTO DE CIÊNCIAS DA VIDA

FACULDADE DE CIÊNCIAS E TECNOLOGIA
UNIVERSIDADE DE COIMBRA

Dimethylaminopyridine Derivatives of Lupane Triterpenoids Acting as Mitochondrial-Directed Agents on Breast Cancer Cells

Telma Sofia Correia Bernardo

2011

DEPARTAMENTO DE CIÊNCIAS DA VIDA

FACULDADE DE CIÊNCIAS E TECNOLOGIA
UNIVERSIDADE DE COIMBRA

Dimethylaminopyridine Derivatives of Lupane Triterpenoids Acting as Mitochondrial-Directed Agents on Breast Cancer Cells

Dissertação apresentada à Universidade de Coimbra para cumprimento dos requisitos necessários à obtenção do grau de Mestre em Biologia Celular e Molecular, realizada sob a orientação científica do Professor Doutor António Matos Moreno (Universidade de Coimbra) e do Doutor Paulo Jorge Oliveira (Universidade de Coimbra).

Telma Sofia Correia Bernardo

2011

This work was conducted in the Center for Neuroscience and Cell Biology, Mitochondrial Toxicology and Disease Group under the supervision of António Matos Moreno, PhD and Paulo Jorge Oliveira, PhD. and funded by research grant PTDC/QUI-QUI/101409/2008.

Some of the contents in this dissertation are part of the following book chapter:

Ana C. Moreira, Nuno G. Machado, Telma C. Bernardo, Vilma A. Sardão, Paulo J. Oliveira (2011) **Mitochondria as a Biosensor for Drug-induced Toxicity – Is It Really Relevant?** In Biosensors for Health, Environment and Biosecurity - Book 2, Andrea Serra, ed. In Tech, Rijeka, Croatia.

Recomeça…
Se puderes,
Sem angústia e sem pressa.
E os passos que deres,
Nesse caminho duro
Do futuro,
Dá-os em liberdade.
Enquanto não alcances
Não descanses.
De nenhum fruto queiras só metade.

E, nunca saciado,
Vai colhendo
Ilusões sucessivas no pomar
Sempre a sonhar
E vendo
Acordado,
O logro da aventura.
És homem, não te esqueças!
Só é tua a loucura
Onde, com lucidez, te reconheças.

Sísifo - Miguel Torga (Diário XIII)

Acknowledgments

First of all, I would like to express my acknowledgments to the Portuguese Foundation for Science and Technology for funding this project.

To Professor António Moreno for the initial support in the laboratory and for the orientation in this work; for the (long) conversations and for the (healthy) discussions; for sharing with me your knowledge in mitochondrial bioenergetics. I do feel so small when I am listening you.

To Doctor Paulo Oliveira[1] for the knowledge, friendship and trust that you gave me. Thank you from the heart.

To Professor Jon Holy (Department of Biomedical Sciences, University of Minnesota Duluth, USA), to Professor Pavel Krazutsky and to his team at Natural Resources Research Institute (University of Minnesota Duluth, USA) for the kindly preparation of the compounds and for ceding me them for the study.

To Doctor Sancha Santos for receiving me always with a smile and for always trying to solve all the setbacks that occur in the laboratory.

To Doctor Romeu Videira for the scientific cooperation.

To Ana Maria Silva for the friendship, tenderness and commitment; for having always a smile in the face and for being always available to help everyone. It is a great pleasure to work side-by-side with you.

To my colleagues in the Mitochondrial Toxicology and Disease group, for all the scientific and non-scientific friendship, especially to Carolina Moreira (thank you for your support, trust and patience) and to Teresa Serafim (thank you for the initial support in my scientific training).

To my friends. I keep in me a little of you.

More than express my acknowledgments- because for you a “Thanks” is not enough- I want to dedicate this work to the people of my life. You know how important you are to me.

[1] Besides all the kicks in the soccer games.

To my mom, dad and brother.

To Vasco.

List of Headings

Abbreviations List

$\Delta\psi_m$ – Mitochondrial Transmembrane Electric Potential
Acetyl-CoA – Acetyl Coenzyme A
ADP – Adenosine Diphosphate
AIF – Apoptosis Inducing Factor
ANT – Adenine Nucleotide Translocase
Apaf-1 – Apoptosis-Protease Activating Factor 1
ATP – Adenosine Triphosphate
Bak – Bcl-2-Antagonist/Killer
Bax – Bcl-2 Associated X Protein
Bcl-2 – B-cell Lymphoma 2
Bcl-xL – B-Cell Lymphoma-Extra Large
BH3-only proteins – Bcl-2 Homology Domain 3-Only Proteins
Bid – Bcl-2 Inhibitor Domain
BSA – Bovine Serum Albumin
Cs A – Cyclosporin A
CypD – Cyclophilin D
Cyt *c* – Cytochrome *c*
Cu/ZnSOD – Cu/Zn- Dependent Superoxide Dismutase
DMAP – Dimethylaminopyridine
DISC – Death-Inducing Signaling Complex
DLC – Delocalized Lipophilic Compounds
DMEM – Dulbecco's Modified Eagle's Medium
DMSO – Dimethylsulfoxide
DNA - Deoxyribonucleic Acid
EGTA – Ethylene glycol-bis(2-aminoethylether)-*N,N,N′,N′*-tetraacetic acid
Endo G – Endonuclease G
ETC – Electron Transport Chain
FCCP – Carbonyl cyanide p-trifluoromethoxyphenylhydrazone
GSH – Glutathione Peroxidase
HEPES – 4-(2-Hydroxyethyl)piperazine-1-ethanesulfonic acid, N-(2-Hydroxyethyl)piperazine-N′-(2-ethanesulfonic acid)
IMS – Intermembrane Space
MIM – Mitochondrial Inner Membrane

MnSOD – Manganese Superoxide Dismutase

MOM – Mitochondrial Outer Membrane

MOMP – Mitochondrial Outer Membrane Permeabilization

MPT – Mitochondrial Permeability Transition

MPTP – Mitochondrial Permeability Transition Pore

NADH – Nicotinamide Adenine Dinucleotide

OXPHOS – Oxidative Phosphorylation

PBS – Phosphate Buffered Saline Solution

PBST – Phosphate Buffered Saline Solution with Tween 20

PCD – Programmed Cell Death

PDH – Pyruvate Dehydrogenase

PiC – Phosphate Carrier

PTP – Permeability Transition Pore

PUMA – p53 Upregulated Modulator of Apoptosis

RCR – Respiratory Control Ratio

ROS – Reactive Oxygen Species

SEM – Standard error of the mean

Smac/Diablo – Second Mitochondria Derived Activator of Caspases/ Direct Inhibitor of Apoptosis-Binding Protein with a Low Isoelectric Point

QSARs – Quantitative Structure-activity Relationships

SRB – Sulforhodamine B

tBid – Truncated Bid

TNF – Tumor Necrosis Factor

TRAIL – Tumor Necrosis Factor-Related Apoptosis-Inducing Ligand

TPP^+ – Tetraphenylphosphonium Ion

VDAC – Voltage-Dependent Anion Channel

Abstract

Cancer is not a unique disease but a generic term used to encompass a set of more than two hundred diseases. Although possessing biological and molecular heterogeneity, cancers share common characteristics such as uncontrolled growth and their increased resistance to apoptosis induction. Mitochondria are the powerhouse of the cells but also their suicidal weapon stores. Therefore, it is not surprising that mitochondria have emerged as intriguing targets for anticancer therapy. Compounds that directly affect mitochondrial functions and trigger apoptosis are considered as promising chemotherapeutics used to eliminate tumor cells. Triterpenoids are a class of natural occurring compounds whose anticancer activity has already documented and linked to apoptosis induction via direct mitochondrial alterations. The objective of the present work was to investigate the potential mitochondrial toxicity induced by novel dimethylaminopyridines of pentacyclic triterpenes derivatives, using isolated hepatic mitochondrial fractions and comparing their effectively as anti-cancer agents in three distinct cell lines.

The present work supports the idea that DMAP triterpenoid derivatives can be promising chemotherapeutic agents since effects were more prominent in cancer vs. non-cancer cells. Assays on isolated hepatic mitochondria showed a multitude of different effects in several targets, although most can induce the mitochondrial permeability transition pore (MPTP). In fact, we can speculate that MPTP induction may be one mechanism by which these compounds cause cell death. Nevertheless, further refinement of the molecules can be expected since mitochondrial toxicity in non-target organs is likely. We also confirm that the test compounds act in different ways according to their number, orientation and position of DMAP groups.

***Keywords**: Triterpene derivatives, mitochondria, cancer cells, transition pore*

Resumo

O cancro não é uma doença particular mas sim um termo genérico que abrange mais de duzentas patologias. Embora exista heterogeneidade a nível molecular e biológico, os diferentes tipos de cancro apresentam características comuns como o crescimento descontrolado e uma maior resistência à indução de apoptose. As mitocôndrias não só são responsáveis pela produção de energia na célula como também encerram alguns factores pró-apoptóticos. Assim, não é de surpreender que as mitocôndrias se tenham tornado alvo de interesse na terapia anticancerígena. Compostos que directamente afectam as funções mitocondriais e que induzam apoptose são considerados quimioterapêuticos promissores para eliminar as células tumorais. Os triterpenóides são uma classe de compostos que existem na natureza cuja acção anticancerígena foi já descrita como estando associada à indução de apoptose por efeitos directos na mitocôndria. O objectivo deste trabalho centrou-se em investigar a potencial toxicidade mitocondrial induzida por novas dimetilaminopiridinas, derivadas de triterpenos pentacíclicos, usando fracções mitocondriais isoladas de fígado e comparando o seu efeito anti-tumoral em três linhas celulares distintas.

Este trabalho sustenta a ideia de que os DMAP derivados de triterpenóides podem ser promissores agentes quimioterapêuticos pois os seus efeitos são mais proeminentes em células cancerígenas que em células normais. Ensaios com mitocôndrias isoladas de fígado mostraram que estes compostos têm efeitos diferentes e alvos também diferentes embora a maioria consiga induzir o poro transitório de permeabilidade mitocondrial. De facto, podemos especular que a indução do poro de permeabilidade transitória mitocondrial pode ser um dos mecanismos pelo qual estes compostos induzem morte celular. No entanto, um aperfeiçoamento das moléculas pode ser esperado uma vez que a toxicidade mitocondrial em outros órgãos é provável. Confirmámos também que os compostos testados actuam de diferentes maneiras de acordo com o número, orientação e posição dos grupos DMAP.

***Palavras-chave**: Derivados de triterpenóides, mitocôndria, células cancerígenas, poro de permeabilidade transitória*.

Introduction

CHAPTER

1

1.1 Mitochondria: Structure and Function

Mitochondria, from the Greek *mito* (thread) and *chondros* (grains) are small organelles that exist as a network in the cytoplasm of eukaryotic cells, performing a variety of important functions including energy production, calcium homeostasis, fatty acid metabolism and heme and pyrimidine biosynthesis [1-3]. Moreover, mitochondria play a critical role in programmed cell death (apoptosis) [1, 4]. Mitochondrial structure comprises two different membranes - the mitochondrial outer membrane (MOM) and the mitochondrial inner membrane (MIM), that functionally separate two distinct compartments, the intermembrane space (IMS) and the mitochondrial matrix [5] (Figure 1, panel B). The outer membrane encloses this organelle and is identical to other cell membranes since it contains cholesterol and is permeable to ions. In counterpart, the inner membrane is rich in cardiolipin (an acidic and hydrophobic phospholipid) and is devoided of cholesterol, being impermeable to ions and small molecules, which require specific transport proteins to move across inner membrane [6]. The inner membrane surrounds the matrix which contains a small circular genome and includes multiple invaginations towards the matrix called *cristae*, where different respiratory complexes (complexes I–IV) and ATP synthase (complex V) responsible for oxidative phosphorylation exist [7].

1.1.1 Organization and Genomics

Also known as mitochondrial *reticulum*, the mitochondrial network continuously moves, fuses and divides in a process tightly regulated by cellular stimuli and disturbances inside this organelle [8]. The shape greatly varies from tissue, developmental and physiological states. Within a cell, the distribution of mitochondria is unequal, depending on the cellular energetic or metabolic requests [9-11]. The overall shape of mitochondrial network results from an equilibrium between fusion and fission events [12]. This events allow the exchange of organelles contents such as membrane lipids, proteins, solutes, metabolites and mitochondrial DNA [8], as well is committed to the electrochemical gradient balance [13] and is crucial to preserve mitochondrial integrity and functionality.

1.1.2 Oxidative Phosphorylation and Energy Production

The available energy within a living cell is performed by a conversion of dietary fats and carbohydrates into reducing equivalents. Mitochondria are the powerhouses of the cell and also execute a key role in other important metabolic pathways. Pyruvate is formed in the cytosol as an end-product of glucose metabolism (glycolysis) and can undergo lactic acid or alcoholic fermentation in the absence of oxygen (anaerobic conditions). Under aerobic conditions, pyruvate can be converted to acetyl coenzyme A (acetyl-CoA) by pyruvate dehydrogenase (PDH) in the mitochondrial matrix [2] that enters in the Krebs cycle, and is oxidized to generate reducing equivalents in the form of NADH and ubiquinol (Figure 1, panel A). Intermediates of the Krebs cycle are also quite important in other metabolic pathways since they are biosynthetic precursors of heme and amino acids [14]. Mitochondria can be either involved in the reduced equivalents production through β-oxidation of fatty acids [15]. The end product of this pathway is, once again, acetyl-CoA that can also enter in the Krebs cycle. All of these equivalents, that are produced by different pathways, are funneled into the electron transport chain (ETC) that is located mostly in mitochondrial *cristae*, and ultimately lead to the production of adenosine triphosphate (ATP) by oxidative phosphorylation (OXPHOS) [7, 16-17] (Figure 1, panel C). The electrons are passed along the chain (OXPHOS complexes I-IV) and the energy derived from them is used to pumps out protons across the inner membrane at complexes I, III and IV, which creates an

electrochemical gradient between both sides of inner membrane. This electrochemical gradient is a proton-motive force that drives the re-entry of protons towards the matrix through complex V (ATP synthase) for ATP synthesis [17]. The ATP that is produced becomes available for the entire cell after the mitochondrial carrier ANT (mitochondrial adenine nucleotide translocase) switched it by a cytosolic ADP. Molecular oxygen is the final electron acceptor, which is reduced to water via a sequential four-electron transfer. However, single electrons that pass across the ETC can escape and perform a single electron reduction of molecular oxygen. This phenomenon occurs continuously even in normal conditions leading to formation of superoxide anion ($O_2^{\bullet -}$).

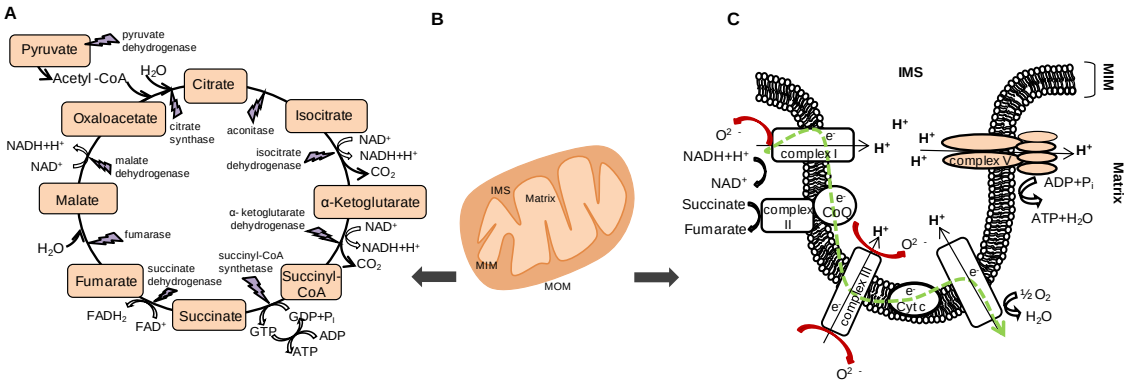

Figure 1: Mitochondria play a critical role in ATP production, biosynthesis, calcium homeostasis and cell death. The figure represents some of these functions: (Panel A) The Krebs cycle occurs in the matrix and supplies reducing equivalents for oxidative phosphorylation, besides participating as intermediate in several biosynthetic pathways. (Panel B) Overall view of mitochondria morphology: The MOM encloses the organelle within the cell; the MIM separates functionally the matrix from the mitochondrial inter-membrane space (IMS). (Panel C) Oxidative phosphorylation: electrons from the Krebs cycle are transferred along the respiratory chain. The energy derived from electron transfer is used to pump out protons across the inner membrane at complexes I, III and IV, creating a proton electrochemical gradient between both sides of inner membrane. This electrochemical gradient forms a proton-motive force that is used to drive the re-entry of protons to the matrix through complex V (ATP synthase) for ATP production [17]. A small amount of electrons can leaks towards the matrix through complex I and complex III performing a one-electron reduction of molecular oxygen forming superoxide anion ($O_2^{\bullet -}$). Figure adapted from [2], with permission.

1.1.3 Reactive Species and Oxidative Stress

"Living with the risk of oxidative stress is a price that aerobic organisms must pay for more efficient bioenergetics" (Skulachev, 1996 *cit in* [18]). Among the reactive species that are produced within a living cell, reactive oxygen species (ROS) are the most significant. Indeed, ROS are produced continuously as a by-product of OXPHOS but mitochondria has an efficient antioxidant network that can counteract detrimental effects of these reactive species and perform the redox balance. Oxidative damage, so-called oxidative stress arises when an imbalance in the redox steady-state occurs and the ROS production exceeds the capacity of the cell to detoxify them. Oxidative stress is largely related with aging [19] and is often associated with various disorders, such as cancer [3].

1.2 The Role of Mitochondria in Cancer

Cancer is not only a definite disease but a generic term used to encompass a set of more than two hundred diseases. Besides biological and molecular heterogeneity of cancers, all share common characteristics. Generally, cancer cells uncontrolled growth and invasive potential are the primary features that describe them but there are more features to be addressed. Six cell-intrinsic hallmarks have been originally proposed by Hanahan and Weinberg in 2000 to define a cancer cell: self-sufficiency in growth signals, insensitivity to antiproliferative signals, acute replicative potential, tissue invasion with metastasis, sustained angiogenesis, and apoptotic resistance [20]. Subsequently, avoidance of the immune response [21], enhanced anabolic metabolism [22] and autophagy inhibition [23] have been proposed as additional features that characterize cancer cells. Eradication of cancer cells by non-surgical resources, ultimately leads to apoptosis [24]. Mitochondria occupy a strategic position between bioenergetic/biosynthetic metabolism and cell death regulation. Since cancer cells are more resistant to cell death induction than their normal counterparts, mitochondria are emerging as idealized targets for anticancer therapy [25]. Indeed, agents that target mitochondria are considered as promising cancer therapeutics even in cancer cells that are resistant to conventional therapies [26-27].

1.2.1 Cell Death

Unlike what was thought until a few years ago, cell death is not a process observed only when cell tissues were injured by external factors. Actually, cell death is an evolutionary conserved and genetically regulated process that is crucial for development, morphogenesis and homeostasis in tissues [28]. Programmed cell death (PCD) was the first designation attributed to this regulated process. Later, Kerr *et al.* introduce the term apoptosis [29] to designate programmed cell death. Apoptosis plays an essential role in the maintenance of homeostasis by eliminating damaged, infected or superfluous cell in a regulated form that minimizes inflammatory reactions and damages in neighboring cells [1, 30]. An imbalance in this process may contribute to the development of many disorders and even the development of cancer [31-32]. Apoptotic cells exhibit specific morphological alterations, including chromatin condensation, nuclear fragmentation, and plasma membrane blebbing. The late stages of apoptosis are characterized by fragmentation of the cell membrane into vesicles (apoptotic bodies) which contain intact cytoplasmatic organelles or fragments of the nucleus. These vesicles are recognized by macrophages, preventing inflammatory responses [28, 33].

There are two main pathways by which a cell can engage apoptosis: extrinsic (or receptor-mediated) apoptotic pathway and intrinsic (or mitochondria-mediated) apoptotic pathway [33] (Figure 2). The apoptotic process is performed by a family of cysteine proteases that are produced as pro-enzymes and must be proteolytically cleaved to produce active forms. These proteases, known as caspases, specifically cleave their substrates at aspartic residues and are categorized into initiators (such as caspases -8 and -9) and effectors or executioners (such as caspases -3 and -7) [1, 31]. The extrinsic pathway is most commonly activated within the immune system and requires the binding of ligand-induced activation of death receptors at the cell surface (such as TNF and TRAIL) [34]. The connection between these specific ligands with their receptors is followed by formation of the death-inducing signaling complex (DISC) that performs the activation of pro-caspase 8 and subsequent activation of downstream executioners caspases [4]. Mitochondria are central players in the intrinsic apoptotic pathway. In addition to its role as a powerhouse of the cell, mitochondria harbors a pool of pro-apoptotic factors which reside in mitochondrial inter membrane space. During the intrinsic pathway, pores are formed in the mitochondrial outer membrane in a process called mitochondrial outer membrane

permeabilization (MOMP). The pro-apoptotic factors such as cytochrome *c* and apoptotic-inducing factor (AIF) that are usually confined to the mitochondrial inner membrane space are released into cytosol [35]. In addition, the opening of the so-called mitochondrial permeability transition pore in the inner mitochondria membrane can also occur during apoptosis, leading to the collapse of $\Delta\psi_m$ and resulting in mitochondrial swelling and rupture of the outer membrane [36]. Although the effects of pro-apoptotic factors that are released in the cytosol is well characterized, the mechanisms underlying the MOMP remains controversial [37]. Induction of the mitochondrial permeability transition can also be considered a more drastic phenomenon which, if widespread to the entire mitochondrial population, can result into severe cell ATP depletion and cell death by necrosis [38].

Several mechanisms have been proposed to explain MOMP, although they generally fall under two classes of mechanisms [32-33]. Each may function under different circumstances. The first model of MOMP involves members of Bcl-2 proteins family and only the MOM permeabilization is implicated (Figure 2). Bcl-2 family comprises three subgroups: the anti-apoptotic Bcl-2 family members such as Bcl-2 ad Bcl-xL, the pro-apoptotic Bax/Bak sub-family and the pro-apoptotic BH3-only proteins such as Bid and Puma. BH3-only proteins link cell death signals to mitochondria and here, the interplay between various members of the Bcl-2 family determines the fate of the cell [39]. A mild change in the dynamic balance of these proteins may result either in inhibition or exacerbation of cell death. As described above, the second model of mitochondrial outer membrane permeabilization, involving the mitochondrial permeability transition (MPT), occurs in response to apoptosis-induced stress and is originally thought to span both inner and outer mitochondrial membranes (Figure 3). In this model, a non-specific channel opens and itself is permeable to solutes up to 1.5 kDa and water [40-41]. The overture of this channel leads to dissipation of mitochondrial transmembrane electric potential ($\Delta\psi_m$) and to the concomitant mitochondrial swelling, which stretches both membranes and burst MOM. The mitochondrial pro-apoptotic factors are released into cytosol and initiates intrinsic apoptotic pathway.

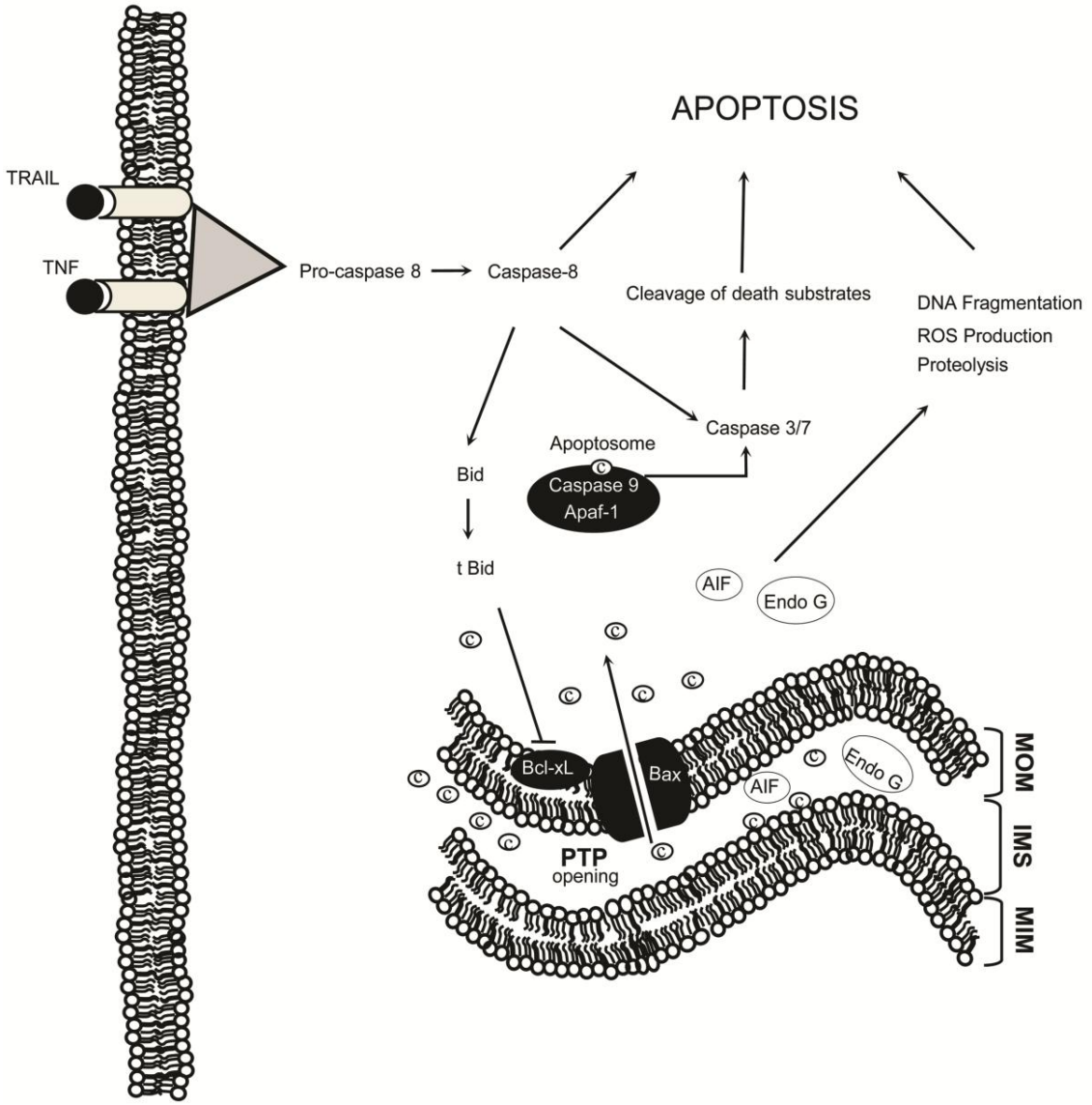

Figure 2: An overview of extrinsic and intrinsic pathways of apoptosis. Extrinsic pathway requires the binding of specific ligands such as TNF and TRAIL to their death receptors at the cell surface which triggers the formation of DISC complex that performs the activation of pro-caspase 8 and subsequent activation of downstream executioners caspases. During intrinsic pathway, pores are formed in the MOM in a process called mitochondrial outer membrane permeabilization (MOMP). One mechanism that might explain this process involves members of Bcl-2 proteins family the anti-apoptotic proteins such as Bcl-2 and Bcl-xL and pro-apoptotic Bax/Bak proteins [35]. A small amount can exist in the MOM but the bulk of these proteins exist in the IMS. In response to internal stimulus, pro-apoptotic proteins are inserted in MOM and oligomerize leading to a formation of channels that allows the release of pro-apoptotic factors. Once in cytosol, cytochrome *c* interacts with Apaf-1 performing the recruitment of pro-caspase 9 and altogether forms the apoptosome complex that activates caspase 9 and leads to activation of effectors caspases 3 and 7. Endo G and AIF go to the nucleus and perform de DNA framentation. The intrinsic and extrinsic pathways can crossroad in mitochondria leading to signal amplification. Figure adapted from [2], with permission.

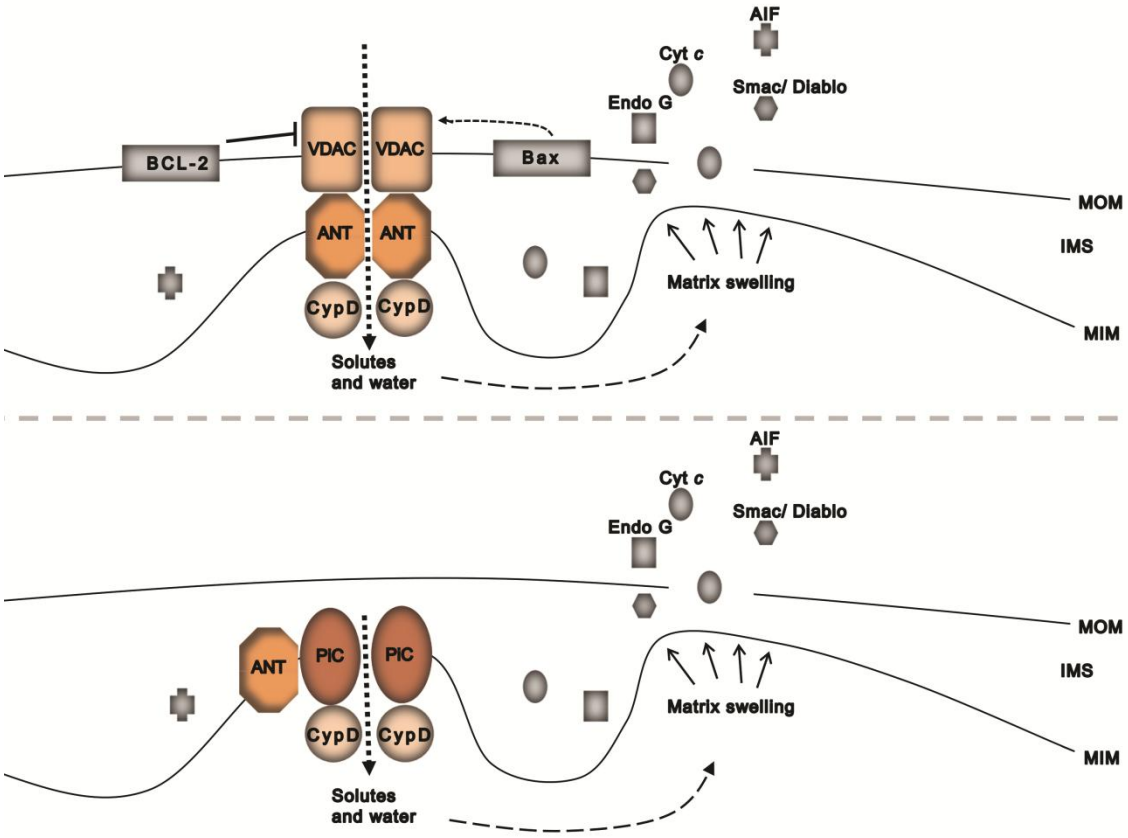

Figure 3: Molecular models for the mitochondrial permeability transition (MPT) pore. On the top: the original model for the MPT pore which considers the assembling of the VDAC (so-called porin) protein in the outer mitochondrial membrane, ANT in the inner mitochondrial membrane and CypD in the matrix [42]. On the bottom: the revised model according to recent findings; VDAC is no longer a component of the PTP (permeability transition pore) and seems that MOM is also not involved in the initiation of this process. Like VDAC, ANT is no longer a component of the pore in this model, but apparently regulates its activity. CypD is the only one that remains as a critical component of this complex. Another protein has been added to the model as a pore-forming unit, the mitochondrial phosphate carrier (PiC) [42]. Although the precise molecular composition of PTP complex is still debated, it is clear that under some circumstances (like an overload of calcium, excess of ROS production) the mitochondrial inner membrane permeability is disrupted. MIM becomes permeable to ions and water causing mitochondrial swelling. Since mitochondrial outer membrane lacks invaginations, mitochondrial swelling breaks MOM and pro-apoptotic factors that were trapped in MIM space are released into cytosol and initiate intrinsic apoptotic pathway [39].

1.2.2 Mitochondrial Alterations in Carcinogesis

Mitochondrial alterations are one of the more recurrent features in cancer cells [43]. The first suggestion about the role of mitochondria in tumor metabolism appeared in 1920's, when Otto Warburg observed higher glucose consumption in tumor cells, even under normoxic conditions [44]. Following this observation, Warburg hypothesized that tumor cells produce most of their ATP by aerobic glycolysis (Warburg effect). Later, other mitochondrial alterations have been reported in cancer cells. Alterations in oxidative phosphorylation resulting from mitochondrial dysfunction, such as mutations in mitochondrial and nuclear genes that encode proteins involved in OXPHOS, have been hypothesized to be involved in tumorigenesis [45]. OXPHOS impairment can enhance ROS production which in turn accelerates the rate of DNA mutation. This scenario has been proposed to be involved in the pathophysiology of cancer. Also, mitochondrial DNA copy number decrease has been associated with resistance to apoptosis and increased invasiveness [46]. The loss-of-function of mitochondrial-specific enzymes like fumarate and succinate dehydrogenase, results in the accumulation of specific metabolites in the cytosol, that can favor the activation of transcription factors such as HIF (hypoxia inducible factor) which in turn can direct metabolism to aerobic glycolysis [47]. Such alterations in cellular metabolism may favor tumor cell growth by increasing the availability of biosynthetic intermediates needed for tumor cells proliferation and adaptation to tumor microenvironments [48].

Another commonly observed difference in mitochondria cancer cells when compared to their normal counterparts is the increased mitochondrial transmembrane electric potential ($\Delta\psi_m$) in the former [49-50]. Mitochondrial transmembrane electric potential is increased to greater negative values (usually -120 to -170 mV, negative inside) which represents a range of ~60mV [51]. Many proposals can explain these differences and include, among others, alterations in mitochondrial respiratory enzyme complexes, electron carriers and in membrane lipid metabolism [52]. Cancer cells exhibit in general an increase in glycolysis and a decrease in oxidative phosphorylation (OXPHOS) activity (Warburg effect) that *per se* can explain the greater mitochondrial transmembrane potential. Reduced OXPHOS activity leads to a build-up of protons in mitochondrial intermembrane space, increasing $\Delta\psi_m$ [49].

1.2.3 Mitochondria as a Pharmacological Target in Cancer Therapy

Despite the diversity of the physical-chemical properties or the intended mechanisms of action, anticancer drugs exert typically cytotoxic effects by initiating intrinsic death pathways that ultimately converge in mitochondria [24]. The main goal of these anticancer drugs is to achieve optimal cytotoxic efficiency and tissue selectivity [53]. In other words, anti-cancer drugs are developed with the expectation that they kill more effectively cancer cells with minimal adverse effects to normal tissues. When classical chemotherapeutic agents cause a primary insult, such as DNA damage, p53 content increase and pro-apoptotic proteins translocate to mitochondria, causing the release of cytochrome *c* and subsequent caspase activation. Frequently, many cancers regress after initial chemotherapy treatments. However, if some of these cancer cells acquired the ability to survive, quite often the cancer returns. Chemoresistant cells have acquired the ability to overcome death signals in different ways, including loss or mutation of p53 and overexpression of anti-apoptotic molecules like Bcl-2 [24]. Therefore, compounds that directly induce mitochondrial intrinsic pathway can theoretically bypass primary or acquired resistance mechanisms that frequently exist or develop towards classical chemotherapeutics [26] (Figure 4). Indeed, mitochondria are emerging nowadays as idealized targets for anticancer therapy [26].

On the other hand, mitochondria form cancer cell exhibit unique features that *per se* offer interesting ground for the development of novel selective anticancer therapeutics. As seen above, mitochondrial transmembrane electric potential is increased at least ~60mV in some cancer cell types. It was already recognized that delocalized lipophilic compounds (DLC) accumulate in mitochondria matrix driven by electrochemical gradient [51]. Some of these DLC are sensitive to higher $\Delta\psi_m$ and selectively accumulate in cancer cells mitochondria. According to the Nernst equation, a range of 60 mV in $\Delta\psi_m$ is sufficient to account for a 10-fold greater accumulation of the cationic compound in malignant cells [49, 54]. Moreover, the greater plasma membrane potential (negative inside) observed in some carcinoma cells when compared to their normal counterpart accounts for further increased DLC accumulation in carcinoma mitochondria [27, 51].

As discussed above, anticancer drugs are developed with the expectation that they are more effectively targeted to malignant cells than to normal cells. Taking advantage of the singular mitochondrial features, the development of drugs that directly exert their function in mitochondria are promising approaches in cancer eradication.

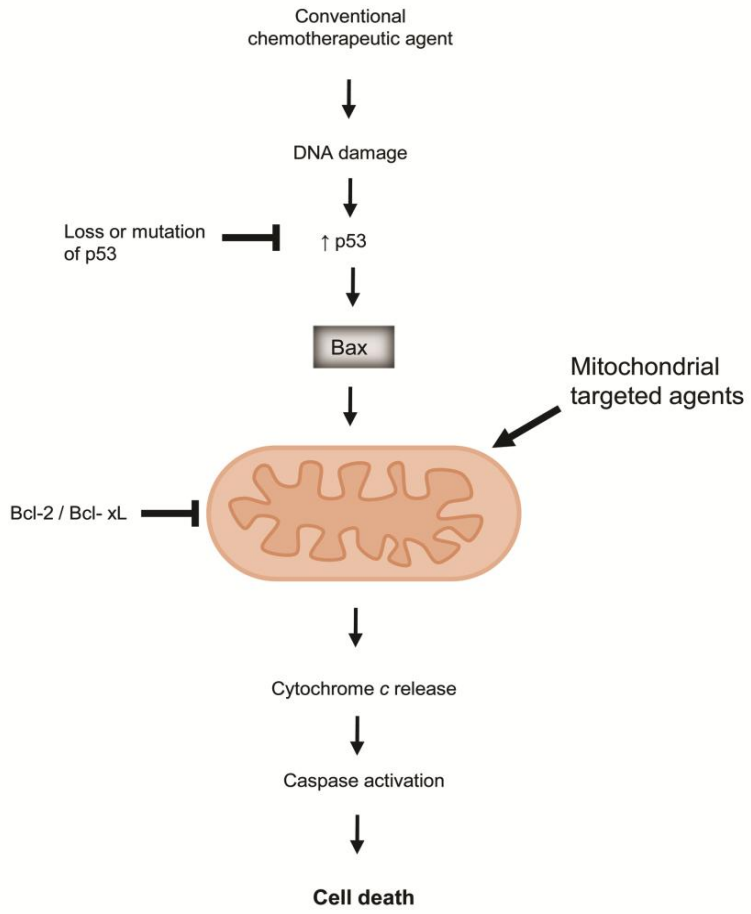

Figure 4: Mitochondria as a main target in cancer therapy [26]. In contrast to many conventional anticancer drugs, which rely on upstream signaling cascades to engage the mitochondrial apoptosis pathway, mitochondria-targeting drugs offer the advantage to act independent of these upstream events that are often blocked in cancers. Adapted from [24].

1.3 Triterpenoids as Anticancer Drugs

Triterpenoids are naturally occurring compounds with ubiquitous distribution. It is believed that their broad occurrence in terrestrial and marine flora is due to their physiological function in defense against plant-pathogens [55]. This has lead to the

expectation that triterpenoids could also act against pathogens that cause human and animal diseases [56]. Indeed, the biological activity of some triterpenoids in mammalian cells, including antiviral [57], antifungal, anti-inflammatory [58] and even antitumor effects has already been documented [59-60]. Betulinic acid is one of these natural compounds that displays notable level of discrimination in promoting apoptosis of melanoma cancer cells [61]. Subsequent studies demonstrate that betulinic acid also exhibits activity in glioma, ovarian carcinoma and cervical carcinoma cell lines [60].

Interestingly, the anticancer activity of some triterpenoids has been linked to their ability to induce apoptosis via direct mitochondrial alterations [62]. Indeed, triterpenoids compounds are emerging as promising in the cancer research. These natural products can largely be extracted from the birch bark, however, the use of these triterpenoids remains quite limited, due to their low solubility, high pH and high molecular weight [56]. Taking advantage of biological activity structures, derivatives of triterpenoids are synthesized to overcome these limitations. Derivatives are positively charged with the main goal to target mitochondrial cancer matrix.

1.4 Aim

Our research group has previously tested a number of dimethylaminopyridine (DMAP) derivatives of lupane triterpenoids on human melanoma cell lines [56]. These compounds induced mitochondrial fragmentation and depolarization, along with an inhibition of cell proliferation. The potency of their effects was correlated with the number, position, and orientation of the DMAP groups. Overall, the extent of proliferation inhibition was shown to mirror the effectiveness of mitochondrial disruption. The present thesis is the follow-up of this previous study, investigating the direct toxicity of some of the DMAP compounds on isolated hepatic mitochondrial fractions in order to identify mitochondrial mechanisms that can explain their cellular effects. We also investigated the same compounds in two human breast cancer cell lines vs. a non-tumor cell line to confirm that the same compounds would have specificity towards the breast tumor cell lines.

Materials and Methods

CHAPTER

2

2.1 General Chemicals

Mitotracker Red CMXRos (#M-7512) and ProLong Gold antifade reagent with DAPI (#P-36931) were obtained from Molecular Probes (Invitrogen, Eugene, OR); Sulforhodamine B (SRB) was obtained from Sigma (St Louis, MO). All other reagents and chemical compounds used were of the greatest degree of purity commercially available. In the preparation of every solution, ultrapure distilled water, filtered by the Milli Q from a Millipore system, was always used in order to minimize as much as possible contamination with metal ions.

2.2 Synthesis and Preparation of the Compounds

Triterpenoid derivatives were produced in the Laboratory of Chemical Extractive Natural Resources Research Institute, University of Minnesota, Duluth, USA by Drs. Pavel Krasutsky and Dmytro Krasutsky. Birch bark lupane triterpenoids betulin and betulinic acid (Figure 5) have been chosen as basic natural precursors for synthesis of dimethylaminopyridine (DMAP) derivatives of pentacyclic triterpenes (Figure 6). Betulin with 99% + purity was isolated from the extract of outer birch bark of *Betula*

papyrifera – the North American commercial birch tree [60] – and betulinic acid was then synthesized from betulin. The compounds were prepared as stock solutions in dimethylsulfoxide (DMSO) and the maximum concentrations added were 2 µg/ml in cells experiments and 6 µg/mg of protein in mitochondrial experiments. The total volume of DMSO was always lower than 0.1% in cell studies and lower than 0.3% in mitochondrial toxicity studies, which had negligible effects in all experiments (data not shown).

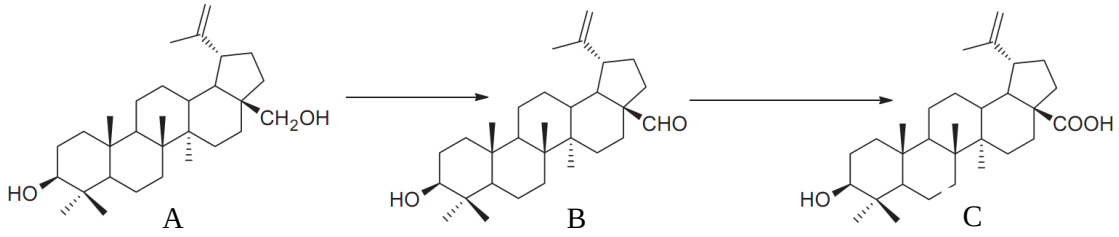

Figure 5: Synthesis of betulinic acid from betulin in a two step process. (A) Birch back lupane triterpenoid betulin isolated from *Betula papyrifera*. (B) Betulinic aldehyde wich is an intermediate product of betulinic acid synthesis. (C) Betulinic acid synthesized from betulin. Adapted from [60], with permission.

2.3 Composition of Solutions

Phosphate buffered saline solution (PBS): 132.0 mM NaCl, 4.0 mM KCl; 1.2 mM NaH_2PO_4. (PBST): PBS with 0.1% Tween 20; 1.4 mM $MgCl_2$; 6.0 mM glucose; 0.1 mM 4-(2-Hydroxyethyl)piperazine-1-ethanesulfonic acid, N-(2-Hydroxyethyl) piperazine-N′-(2-ethanesulfonic acid) (HEPES). The trypan blue was used as a 0.04% (w/v) solution in PBS.

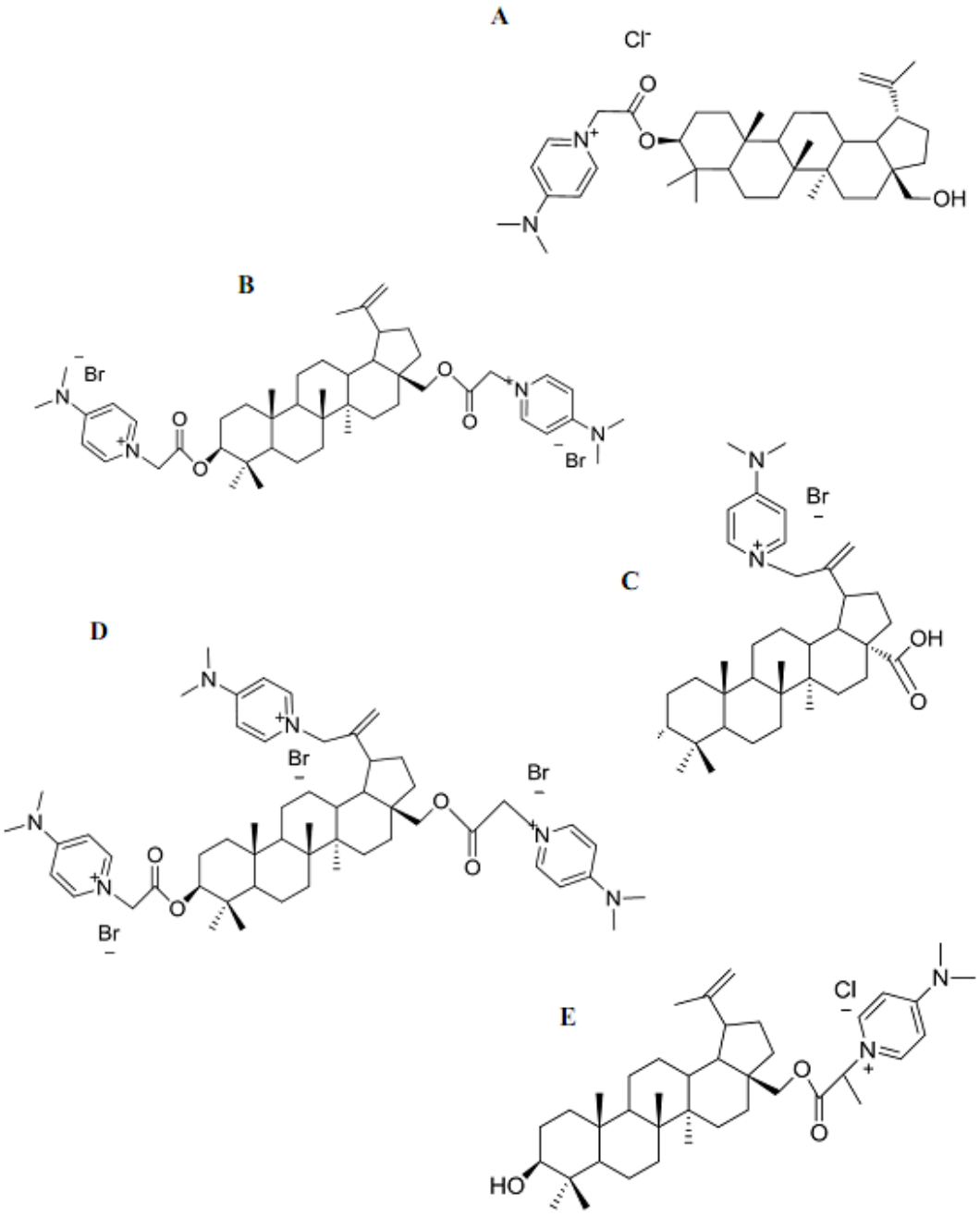

Figure 6: DMAP compounds synthesized from betulin an betulinic acid. (A) DK 43: Lup-20-(29)-ene-3β-(4'-Dimethylaminopyridiniumacetoxy) chloride; B) OK 221: Betulin 3β,28-di[(4'-Dimethylaminopyridinium-1'-yl)acetoxy] bromide; (C) OK 236: Betulinic acid 28-(4'-Dimethylaminopyridinium-1'-yl) bromide; (D) OK 208: Betulin 30-[4'-(Dymethylamino)pyridinium-1'-yl]-3β,28-di[4'-(Dimethylamino)pyridinium-1-yl acetoxy)] tribromide; (E) OK 198: 28-(4'-Dimethylaminopyridinium-1'-acetoxy)-3β-hydroxylup-20(29)-ene chloride. Structures were kindly provided by Dr. Pavel Krasutsky from the University of Minnesota, Duluth, USA.

2.4 Animal Handling

Male Wistar-Han rats (8-10 weeks of age) were housed in our accredited animal colony (Laboratory Research Center, Faculty of Medicine, University of Coimbra) in type III-H cages (Tecniplast, Italy) and maintained in specific environmental requirements: 22° C, 45–65% humidity, 15–20 changes/hour ventilation, 12h artificial light/dark cycle, noise level < 55 dB. Rats had free access to standard rodent food (4RF21 GLP certificate, Mucedola, Italy) and water (acidified at pH 2.6 with HCl to avoid bacterial contamination). This research procedure was carried out in accordance with European Requirements for Vertebrate Animal Research and according to the ethical standards for animal manipulation at the Center for Neuroscience and Cell Biology.

2.5 Cell Culture

MCF-7 (HTB-22, ECACC, United Kingdom) and Hs 578T (HTB-125, ATCC, Manassas, VA, USA), breast cancer cell lines, as well as BJ normal fibroblasts (CRL-2522, ATCC, Manassas, VA, USA), were cultured in monolayers in Dulbecco's modified Eagle's medium (DMEM), supplemented with 1.8 g/l sodium bicarbonate, 10% fetal bovine serum, and 1% of penicillin-streptomycin in 75 cm^2 tissue culture flasks at 37° C in a humidified atmosphere of 5% CO_2. Cells were fed every 2–3 days, and sub-cultured once they reached 70–80% of confluence. BJ fibroblasts were only used between passage 10 and 25.

2.6 Cell Proliferation Measurement

Sulforhodamine B assay was conducted in order to evaluate the cytotoxic effects of Triterpenoids derivatives in tumor and nontumor cell lines, as described by [63]. The human fibroblast cell line BJ and the human breast cancer cell line Hs 578T were seeded at a density of $1x10^4$ cell/ml in 48-well plates (final volume of 500 µl/well). The human breast cancer cell line MCF-7 was seeded at a density of $5x10^3$ cells/ml under the same conditions. The test compounds at various concentrations (0.125 µg/ml;

0.25 µg/ml; 0.5 µg/ml; 1 µg/ml; 2 µg/ml) were added to each well one day after seeding and were incubated for 24h, 48h and 96h. Following treatment, the incubation media were removed and cells were fixed in 1% acetic acid in ice-cold methanol for at least 30 min. The cells were then incubated with 0.5% (wt/vol) SRB dissolved in 1% acetic acid for 1h at 37° C. Unbound dye was removed with 1% acetic acid. Dye bound to cell proteins was extracted with 10 mM Tris base solution, pH 10, and the optical density of the solution was measured in VICTOR X3 Multilabel Plate Reader (Perkin Elmer, Inc.) at 540 nm. The amount of released dye is proportional to the number of cells present in the sample and is a reliable indicator of cell proliferation [64]. The results were expressed as a percentage of control (non-treated) cells, taken as 100%, to equalize for different growth rates between cell lines.

2.7 Epifluorescence Microscopy

For detection of morphological alterations in chromatin condensation and mitochondrial network distribution cells were seeded in six-well plates containing glass coverslips (final volume of 2 ml/well at the same density described in cell proliferation measurement) and allowed to attach for 24h. The human breast cancer cell lines and the untransformed normal fibroblast line were then treated with desired concentrations of test compounds for 48h and 96h. Thirty minutes prior the end of the time exposure, the cultures were incubated with Mitotraker Red (7.3 nM) at 37° C in the dark, washed with cold PBS and fixed with ice cold absolute methanol overnight at -20º C. The cells were then gently rinsed three times with PBST 5 minutes in the dark, at room temperature. Glass coverslips were removed from the wells and placed on glass slides with a drop of mounting media with DAPI. The images were obtained using a 63x objective in a Zeiss Axioskop 2 Plus microscope.

2.8 Isolation of Rat Hepatic Mitochondria

Mitochondria were isolated from the livers of male Wistar rats by conventional differential centrifugation [65]. Rats were killed by decapitation and the livers were harvested, minced and washed in ice-cold buffer medium containing 250 mM

sucrose, 10 mM HEPES (pH 7.2), 1 mM EGTA, and 0.1% lipid-free BSA. Tissue fragments were quickly homogenized with a motor-driven Teflon Potter homogenizer in the presence of ice-cold isolation medium (7 g/50 ml). Hepatic homogenate was centrifuged at 800g for 10 min (Sorvall RC6 centrifuge) at 4° C and mitochondria were recovered from the supernatant by centrifugation at 10,000g for 10 min. The mitochondrial pellet was resuspended using a paintbrush and centrifuged twice at 10,000g for 10 min before obtaining a final mitochondrial suspension. EGTA and BSA were omitted from the final washing medium, which was adjusted to pH 7.2. Protein content was determined by the biuret method [66], using bovine serum albumin (BSA) as a standard.

2.8.1 Measurement of Mitochondrial Oxygen Consumption

Oxygen consumption of isolated hepatic mitochondria was polarographically monitored with a Clark-type oxygen electrode connected to a suitable recorder in a 1 ml temperature-controlled, water-jacketed, and closed chamber with constant magnetic stirring [67]. The reactions were carried out at 30 °C in 1 ml of standard respiratory medium with 1 mg of hepatic mitochondria. Mitochondrial respiratory medium comprised 130 mM sucrose, 50 mM KCl, 2.5 mM $MgCl_2$, 5 mM KH_2PO_4 , 0.1 mM EGTA and 5 mM HEPES (adjusted at pH 7.2). The triterpenoid derivative compounds were preincubated with 1 mg mitochondria for 1 minute before adding the respiratory substrate. This incubation period was carried out to ensure the complete internalization of the compound on the membrane due to its lipophilic characteristic. The respiratory substrates, glutamate/malate (10 mM/ 5mM) or succinate (5 mM) plus rotenone (3 µM), were added to the medium to energize mitochondria, while ADP (187.5 nmol/mg protein) was used to induce state 3. In order to block proton influx through the ATP synthase under state 4 respiration, 1µg oligomycin was added to the system. To uncouple respiration and measure the maximal electron transfer rate through the respiratory chain, 1 µM Carbonyl cyanide p-trifluoromethoxyphenylhydrazone (FCCP) was added. The respiratory control ratio (RCR) is a measure of oxidative phosphorylation coupling and is calculated as the rate between state 3 and state 4. The ADP/O ratio is indicative of the efficiency of oxidative phosphorylation [68]. Both indexes were determined according to Chance

and Williams, 1956 [69]. Respiration rates were calculated considering an air saturated water oxygen concentration of 236 µM, at 30º C.

2.8.2 Measurement of Mitochondrial Transmembrane Electric Potential ($\Delta\psi_m$)

The mitochondrial transmembrane electric potential ($\Delta\Psi_m$) of isolated hepatic mitochondria was monitored indirectly in a 1 ml thermostated, water-jacketed, open chamber with constant magnetic stirring, using an ion-selective electrode to measure the distribution of tetraphenylphosphonium (TPP^+) according to previously established methods [70]. The reference electrode was $Ag/AgCl_2$. Mitochondrial protein (1 mg) was suspended in reaction medium composed of 130 mM sucrose, 50 mM KCl, 2.5 mM $MgCl_2$, 5 mM KH_2PO_4 , 0.1 mM EGTA and 5 mM HEPES (pH 7.2, 30° C), and supplemented with 3 µM TPP^+. Triterpenoid derivative compounds were added to mitochondria for 1 minute to allow complete internalization of the compound, followed by 5 mM glutamate/2.5 mM malate or 5 mM succinate plus 3 µM rotenone. In order to initiate state 3, ADP (125 nmol/mg protein) was added. Valinomycin (0.2 µg) leads to a complete collapse of $\Delta\Psi_m$ and was added at the end of all experiments to confirm if test compounds interfere with the electrode. Assuming a Nernst distribution of the ion across the membrane electrode, the equation proposed by Kamo et al.[71] yielded the values for transmembrane electric potential.

2.8.3 Effects of the Compounds on the MPT: Evaluation of the $\Delta\Psi_m$ Fluctuations

The phenomenon of the mitochondrial permeability transition (MPT) takes place when a large amount of Ca^{2+} is accumulated by mitochondria in the presence of an inducing agent (Pi). The induction of the MPT pore leads to mitochondrial depolarization. The $\Delta\Psi_m$ fluctuations associated with the uptake of calcium and the induction of the MPT pore were followed with a TPP^+-selective electrode (as described above), in an open thermostated water-jacketed reaction chamber with magnetic stirring, at 30º C. Mitochondria (1mg) were suspended in 1 ml of swelling medium consisting of 200 mM sucrose, 10 mM Tris-MOPS (pH 7.2), 10 µM EGTA, 1mM KH_2PO_4, 3 µM rotenone,

supplemented with 3 μM TPP^+. The mitochondria were energized with 5 mM succinate. Hepatic mitochondria were incubated with the test compounds during 1 minute before the respiratory substrate to guarantee their total internalization. Two aliquots of calcium ($CaCl_2$) were added to the reaction medium in the assays ranged from 40 nmol to 60 nmol, depending on mitochondrial preparations. As a control, cyclosporin A (1 μM), a specific MPT pore inhibitor [72], was preincubated with the mitochondrial preparation in the presence of the highest concentration of the tested compounds observed to induce mitochondrial swelling. Another control, with FCCP ($25x10^{-3}$ nmol) was performed in order to induce a small reduction in mitochondrial transmembrane potential. Once again, FCCP was incubated with mitochondrial suspension before calcium addition.

2.8.4 Effects of the Compounds on the MPT: Measurement of Mitochondrial Swelling

The induction of the mitochondrial permeability transition (MPT) pore leads to mitochondrial swelling, which can be estimated by changes in light scattering of the hepatic mitochondrial suspension [73]. The turbidity of the mitochondrial suspension was measured at 540 nm in a Lambda 45 UV/VIS Spectrometer (Perkin Elmer, Inc.). Mitochondrial protein 0.5 mg/ml (final volume of 2 ml) was incubated 1 minute at 30º C in swelling medium containing 200 mM sucrose, 10 mM Tris-MOPS (pH 7.2), 10 μM EGTA, 1 mM KH_2PO_4, 3 μM rotenone, and 5 mM succinate in the presence of the triterpenoids derivative compounds under study. Mitochondrial swelling was induced by adding $CaCl_2$ (ranged from 40nmol to 60nmol depending on mitochondrial preparation) to the system. As a control, 1 μM Cs A, a specific MPT pore inhibitor [72], was incubated with the mitochondrial preparation in the presence of the highest concentration of the test compound observed to induce mitochondrial swelling.

2.9 Statistical Analysis

Data was loaded to the GraphPad Prism 5.0 program (GraphPad Softwere, Inc.) and all results are expressed as means ± standard error of the mean (SEM) and evaluated by one-way ANOVA followed by Bonferroni multiple comparison tests. Values with $p<0.05$ were considered as statistically significant.

Results

CHAPTER

3

3.1 Effect of DMAP Triterpenoid Derivatives on BJ, Hs 578T and MCF-7 Cell Lines Proliferation

To evaluate whether DMAP triterpenoid derivatives inhibit cell proliferation, two human breast cancer cell lines (Hs 578T and MCF-7) and one non-neoplasic human fibroblast cell line (BJ) were incubated in the absence and presence of increasing concentrations of these compounds (0.125, 0.25, 0.5, 1 and 2 µg/ml) for 24, 48 and 96 hours. As shown in figure 7, **OK 198** does not affect cell proliferation of control cell line (BJ) for any concentration or time point in study. In contrast, this triterpenoid derivative inhibits the proliferation of MCF-7 cell line at all concentrations and time points tested. For the Hs 578T cell line, a decrease in cell growth is observed only for some conditions: at 24h (1 µg/ml), 48h (concentrations ranging from 0.5 µg/ml to 2 µg/ml) and for all concentrations at 96h which means that, for this cell line, their effect is more dependent on time exposure than on the compound concentration because for 96h all concentrations inhibit cell proliferation. Similarly to what happened with **OK 198** in BJ fibroblasts, **OK 208** (Figure 8) also did not have any effect on cell proliferation but it shows an inhibition of cell proliferation on Hs 578T and MCF-7 cell line for the highest concentrations and longer time exposure. In this case, **OK 208**

have an effect in MCF-7 cell line that is more dose-dependent than time-dependent. Cell proliferation in BJ cells is not dissimilar from the control in **DK 43** presence (Figure 9) except for the highest concentration at 48 and 96 hours. In the Hs 578T cell line there is an inhibition immediately visible from the second lowest concentration (0.125 µg/ml) at 48 hours and this inhibition is observed for all the concentrations in study at the 96 hours time point. Therefore, its effect is more time dependent than dose-dependent. The other breast cancer cell line (MCF-7) shows a decrease in cell growth at 24 hours for the maximum concentration (2 µg/ml) and has no effects in the lowest concentration (0.125 µg/ml) at 48 hours. Surprisingly, for 96 hours, it appears that MCF-7 cells can recover from the inhibition of cell proliferation registered at 48 hours for 0.25 and 0.5 µg/ml concentrations. **OK 236** (Figure 10) is the only triterpenoid derivative in test that does not present any alteration in cell growth for any time exposure or compound concentration. In turn, **OK 221** (Figure 11) seem to have the most inhibitory power in cell proliferation when compared with other tested compounds. Its effect is denoted for all concentrations range and time exposure for breast cancer cell lines (Hs 578T and MCF-7) and also for the maximum concentration (2 µg/ml) at 24h and for all concentrations at 48 and 96h in BJ normal fibroblasts. Thus, the effect of **OK 221** is notably dose-dependent. It must be noted that the present technique cannot conclude if the effect of DMAP triterpenoid derivatives is due to an increase in cell death induction or due to cell cycle arrest.

OK 198

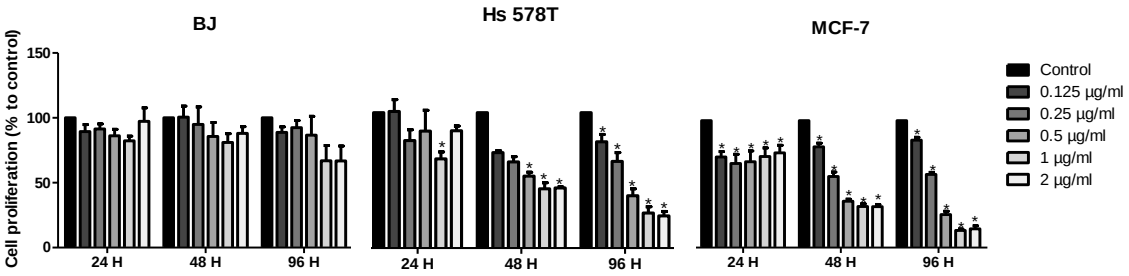

Figure 7: Effect of **OK 198** triterpenoid derivative on cell proliferation of one normal human fibroblast cell line (BJ) and two human breast cancer cell lines (Hs 578 T and MCF-7). Cells were seeded (see Materials and Methods section for further details) and incubated with **OK 198** 24 hours later, at various concentrations during 24, 48 and 96 hours. Cell proliferation assay was accessed at each time by the SRB colorimetric assay. Data are means ± SEM of five independent experiments and are expressed as % control values. * $p < 0.05$ vs. control for the same time point.

OK 208

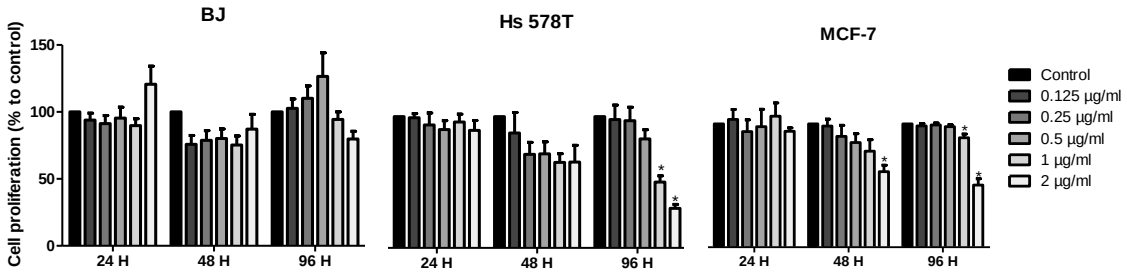

Figure 8: Effect of **OK 208** triterpenoid derivative on cell proliferation of one normal human fibroblast cell line (BJ) and two human breast cancer cell lines (Hs 578 T and MCF-7). Cells were seeded (see Materials and Methods section for further details) and incubated with **OK 208** 24 hours later, at various concentrations during 24, 48 and 96 hours. Cell proliferation assay was accessed at each time by the SRB colorimetric assay. Data are means ± SEM of five independent experiments and are expressed as % control values. * $p < 0.05$ vs. control for the same time point.

DK 43

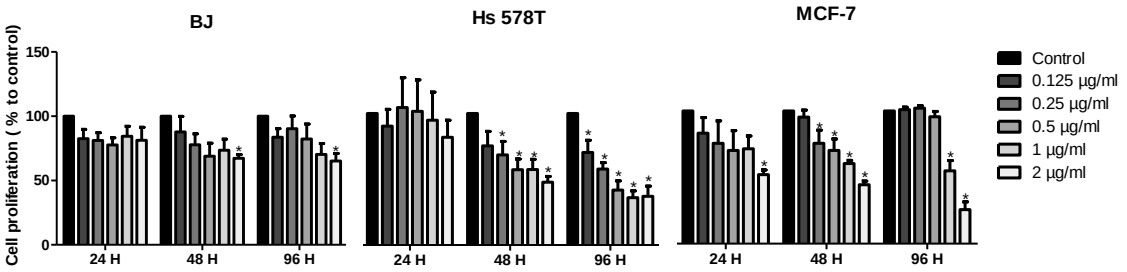

Figure 9: Effect of **DK 43** triterpenoid derivative on cell proliferation of one normal human fibroblast cell line (BJ) and two human breast cancer cell lines (Hs 578 T and MCF-7). Cells were seeded (see Materials and Methods section for further details) and incubated with **DK 43** 24 hours later, at various concentrations during 24, 48 and 96 hours. Cell proliferation assay was accessed at each time by the SRB colorimetric assay. Data are means ± SEM of five independent experiments and are expressed as % control values. * $p < 0.05$ vs. control for the same time point.

OK 236

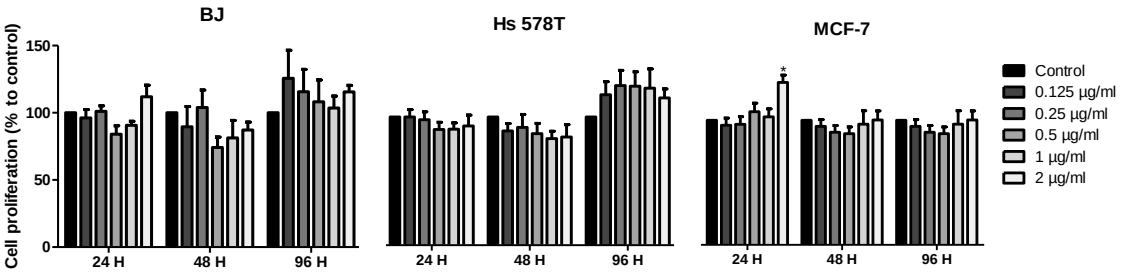

Figure 10: Effect of **OK 236** triterpenoid derivative on cell proliferation of one normal human fibroblast cell line (BJ) and two human breast cancer cell lines (Hs 578 T and MCF-7). Cells were seeded (see Materials and Methods section for further details) and incubated with **OK 236** 24 hours later, at various concentrations during 24, 48 and 96 hours. Cell proliferation assay was accessed at each time by the SRB colorimetric assay. Data are means ± SEM of five independent experiments and are expressed as % control values. * $p < 0.05$ vs. control for the same time point.

OK 221

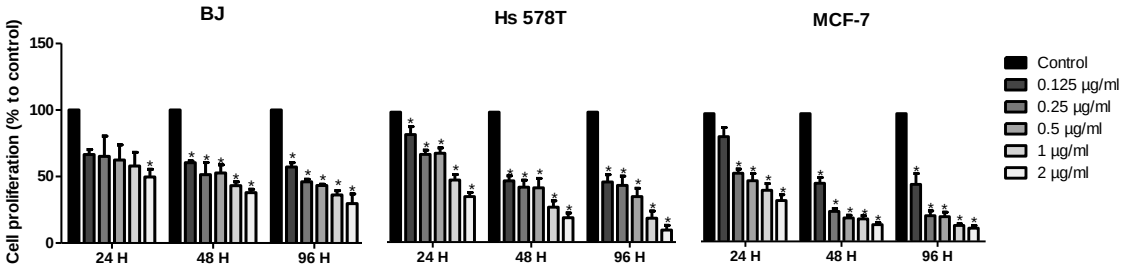

Figure 11: Effect of **OK 221** triterpenoid derivative in cell proliferation of one normal human fibroblast cell line (BJ) and two human breast cancer cell lines (Hs 578 T and MCF-7). Cells were seeded (see Materials and Methods section for further details) and incubated with **OK 221** 24 hours later, at various concentrations during 24, 48 and 96 hours. Cell proliferation assay was accessed at each time by the SRB colorimetric assay. Data are means ± SEM of five independent experiments and are expressed as % control values. * $p < 0.05$ vs. control for the same time point.

3.2 Degree of Mitochondrial Depolarization Caused by DMAP Triterpenoid Derivatives on Breast Cancer Lines and BJ Fibroblasts

In order to better understand the results of the SRB assay and to investigate if DMAP triterpenoid derivatives present mitochondrial toxic effects (observed as mitochondrial depolarization) and cause apoptotic nuclear alterations, a single concentration that does not seem to cause a large extension of cell growth inhibition at 48 and 96 hours was chosen to treat cell lines. Thirty minutes prior to the end of incubation period, cells were incubated with Mitotracker Red (7.3 nM) that is incorporated by mitochondria in live cells dependent upon their mitochondrial membrane potential. Cells were also labeled with the nuclear fluorescent dye DAPI. The results show that **OK 236** triterpenoid derivative (Figure 12 to 17) did not have any visible effect on mitochondria polarization or nuclear morphology in any of the cell lines in study for the concentration (2 µg/ml) and time exposure chosen. In turn, **OK 208** (2 µg/ml), **DK 43** (1 µg/ml) and **OK 221** (0.125 µg/ml) has a strong effect on mitochondrial depolarization for these concentrations in normal BJ fibroblasts (Figure 12 and 13) and in both cancer cell lines (Figure 14 to 17) after 48 and 96 hours of incubation. For the MCF-7 cell line, some apoptotic-like nuclei can be observed after 96 hours of time exposure in **OK 208** and **DK 43** -treated groups (Figure 17). Interestingly, **OK 198** (0.5 µg/ml) induces a mild mitochondrial fragmentation in BJ fibrobaslts for this concentration and exposure times (Figure 12 and 13) although mitochondria still

remains polarized. For both neoplasic cell lines for 48h (Figure 14 and 16) and for 96h (Figure 15 and 17) mitochondria suffer profound fragmentation and depolarization.

3.3 DMAP Triterpenoid Derivatives Effects on Isolated Hepatic Mitochondria: Evaluation of the Mitochondrial Oxygen Consumption

To test whether DMAP triterpenoid derivatives interfere with mitochondrial respiratory parameters, both glutamate/malate (substrate for complex I) and succinate (substrate for complex II) were used for mitochondrial energization in the absence and presence of increasing concentrations (3 and 6 µg/mg of protein) of the compounds (Figure 23). A typical recording of the effect of each one of the tested compounds on mitochondrial oxygen consumption is represented in figures 18 to 22. The triterpenoid derivative **OK 198** seems to exert direct effects in ATP synthase Fo subunit (for selected concentrations) since the increase observed in state 2 and state 4 was not visible when this specific subunit was inhibited (state oligomycin). More, this effect appears to be ATP-dependent because state 4 is further increased when compared to state 2. The increase in ADP/O ratio and the tendency to an increase in mitochondrial depolarization can further confirm this previous result (Table 1). **OK 208**, **DK 43** and **OK 236** triterpenoid derivatives did not interfere with any mitochondrial respiration parameters for selected concentrations except for the RCR ratio parameter that was decreased in the presence of the higher concentration of **OK 208** and **OK 236**. The most powerful compound in cell proliferation (SRB) assays, **OK 221**, has also proved to be the most powerful in mitochondrial respiration studies. In fact, **OK 221** acts in respiratory chain in both glutamate-malate and succinate-energized mitochondria since maximal respiration are decreased in the presence of FCCP (Figure 23). **OK 221** also increases passive flux of protons through mitochondrial inner membrane as shown by the mitochondrial respiration increase when ATP synthase Fo subunit is blocked by oligomycin (state oligomycin). State 2, state 3 and state 4 respiratory parameters confirm the same trend of results. The value for the RCR ratio of the control group denotes a good mitochondrial preparation, which is further confirmed by de ADP/O ratio values.

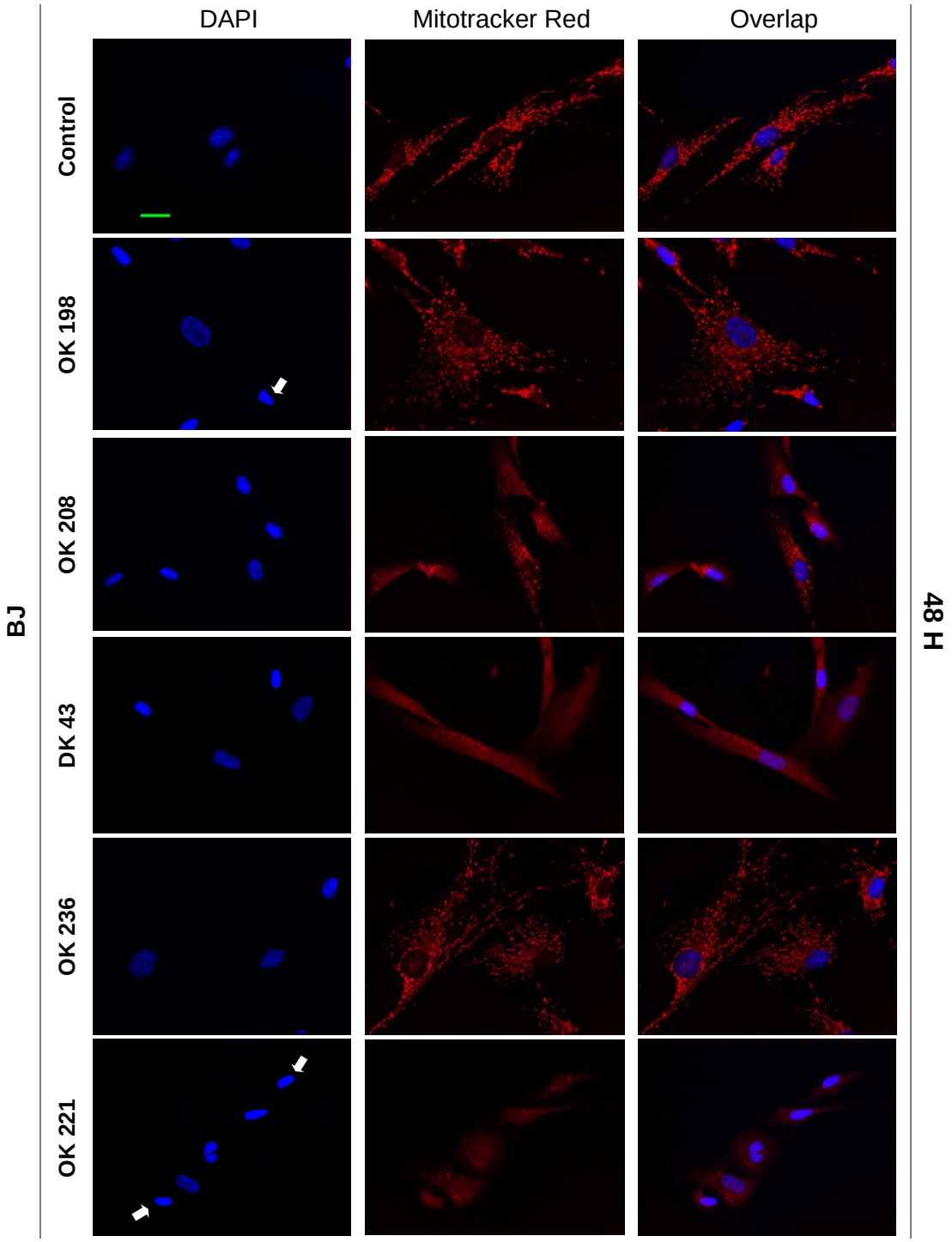

Figure 12: Epifluorescence micrographs showing the effect of DMAP triterpenoid derivatives on nuclear morphology and mitochondrial polarization in BJ cell line after 48 hours of time exposure. Cells were seeded (see Materials and Methods) and incubated 24 hours later at various concentrations (**OK 221**: 0.125 µg/ml; **OK 198**: 0.5 µg/ml; **DK 43**: 1 µg/ml; **OK 208** and **OK 236**: 2 µg/ml). Thirty minutes before the end of incubation period (48 h) cells were incubated with Mitotracker Red (7.3 nM). Cells were also labeled with nuclear fluorescent dye (DAPI) prior microscope visualization. Images of DAPI and Mitotracker labeling (left and central panel, respectively) were obtained with a Zeiss Axioskop 2 Plus microscope. The right panel corresponds to an overlapping of DAPI and Mitotracker staining. The white arrows indicate apoptotic-like nuclei and the green bar represents 20µm. These results are representative of two independent experiments.

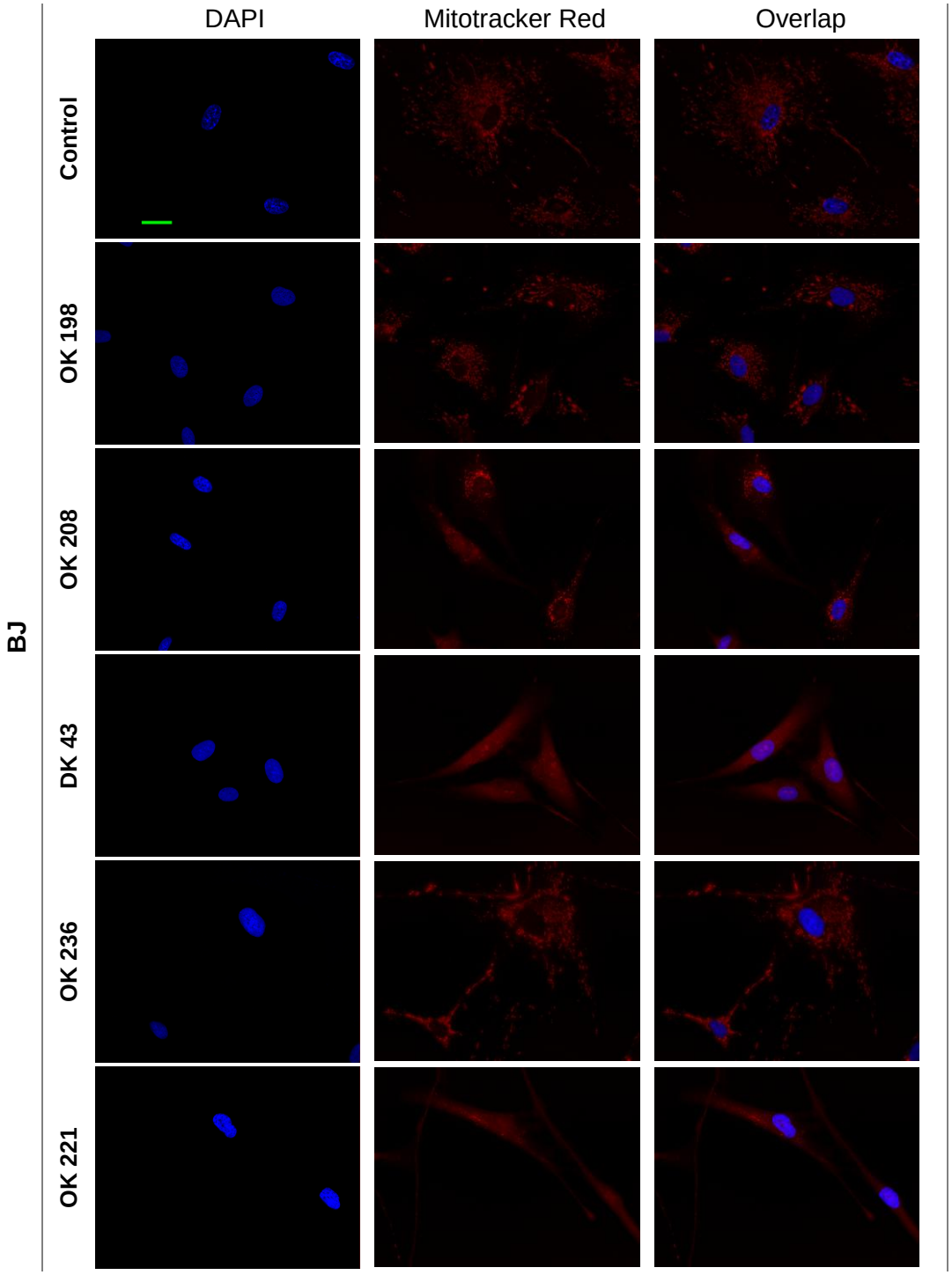

Figure 13: Epifluorescence micrographs showing the effect of DMAP triterpenoid derivatives on nuclear morphology and mitochondrial polarization in BJ cell line after 96 hours of time exposure. Cells were seeded (see Materials and Methods) and incubated 24 hours later at various concentrations (**OK 221**: 0.125 µg/ml; **OK 198**: 0.5 µg/ml; **DK 43**: 1 µg/ml; **OK 208** and **OK 236**: 2 µg/ml). Thirty minutes before the end of incubation period (96 h) cells were incubated with Mitotracker (7.3 nM). Cells were also labeled with nuclear fluorescent dye (DAPI) prior microscope visualization. Images of DAPI and Mitotracker labeling (left and central panel, respectively) were obtained with a Zeiss Axioskop 2 Plus microscope. The right panel corresponds to an overlapping of DAPI and Mitotracker staining. The green bar represents 20µm. These results are representative of two independent experiments.

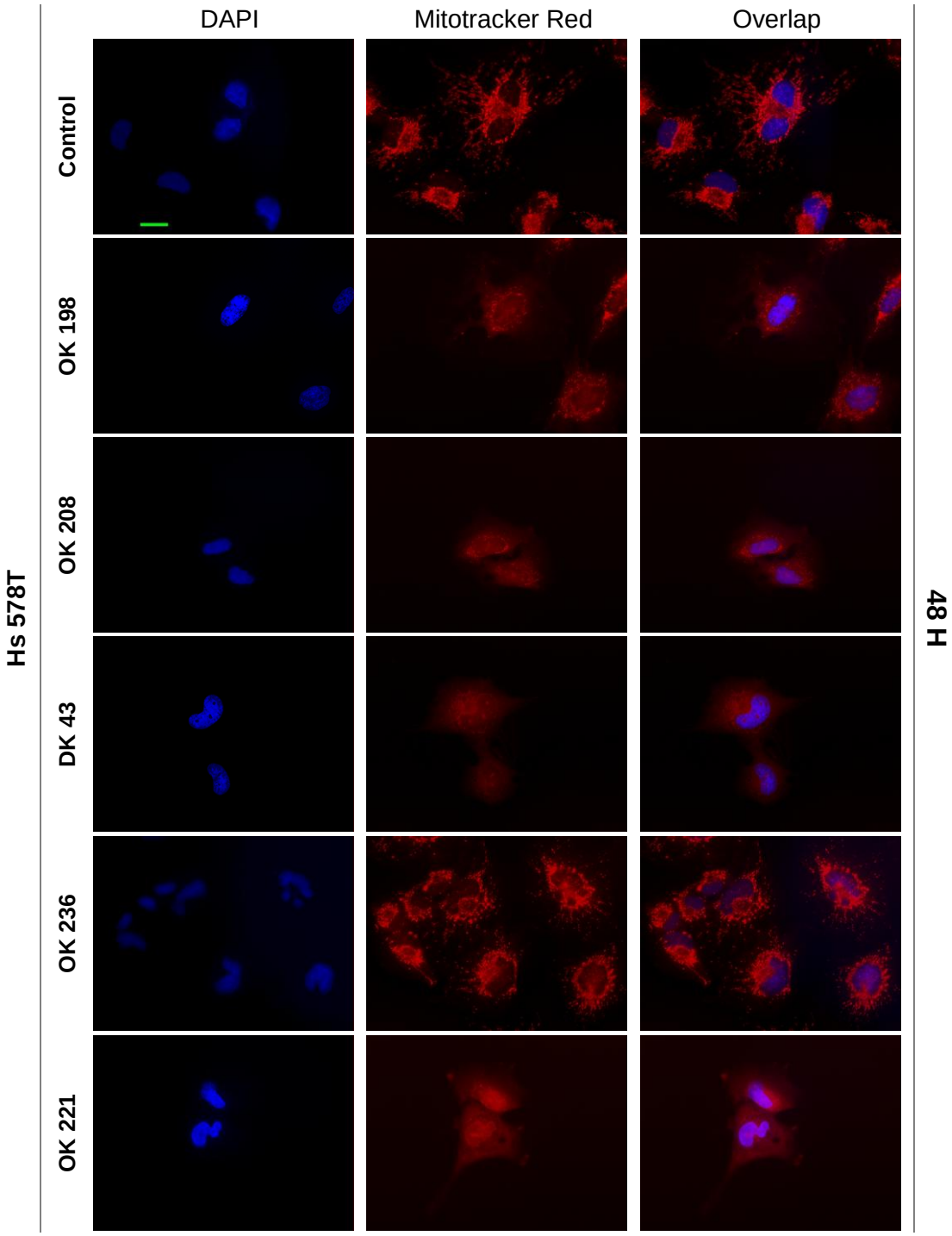

Figure 14: Epifluorescence micrographs showing the effect of DMAP triterpenoid derivatives on nuclear morphology and mitochondrial polarization in Hs 578T cell line after 48 hours of time exposure. Cells were seeded (see Materials and Methods) and incubated 24 hours later at various concentrations (**OK 221**: 0.125 µg/ml; **OK 198**: 0.5 µg/ml; **DK 43**: 1 µg/ml; **OK 208** and **OK 236**: 2 µg/ml). Thirty minutes before the end of incubation period (48 h) cells were incubated with Mitotracker Red (7.3 nM). Cells were also labeled with nuclear fluorescent dye (DAPI) prior microscope visualization. Images of DAPI and Mitotracker labeling (left and central panel, respectively) were obtained with a Zeiss Axioskop 2 Plus microscope. The right panel corresponds to an overlapping of DAPI and Mitotracker staining. The green bar represents 20µm. These results are representative of two independent experiments.

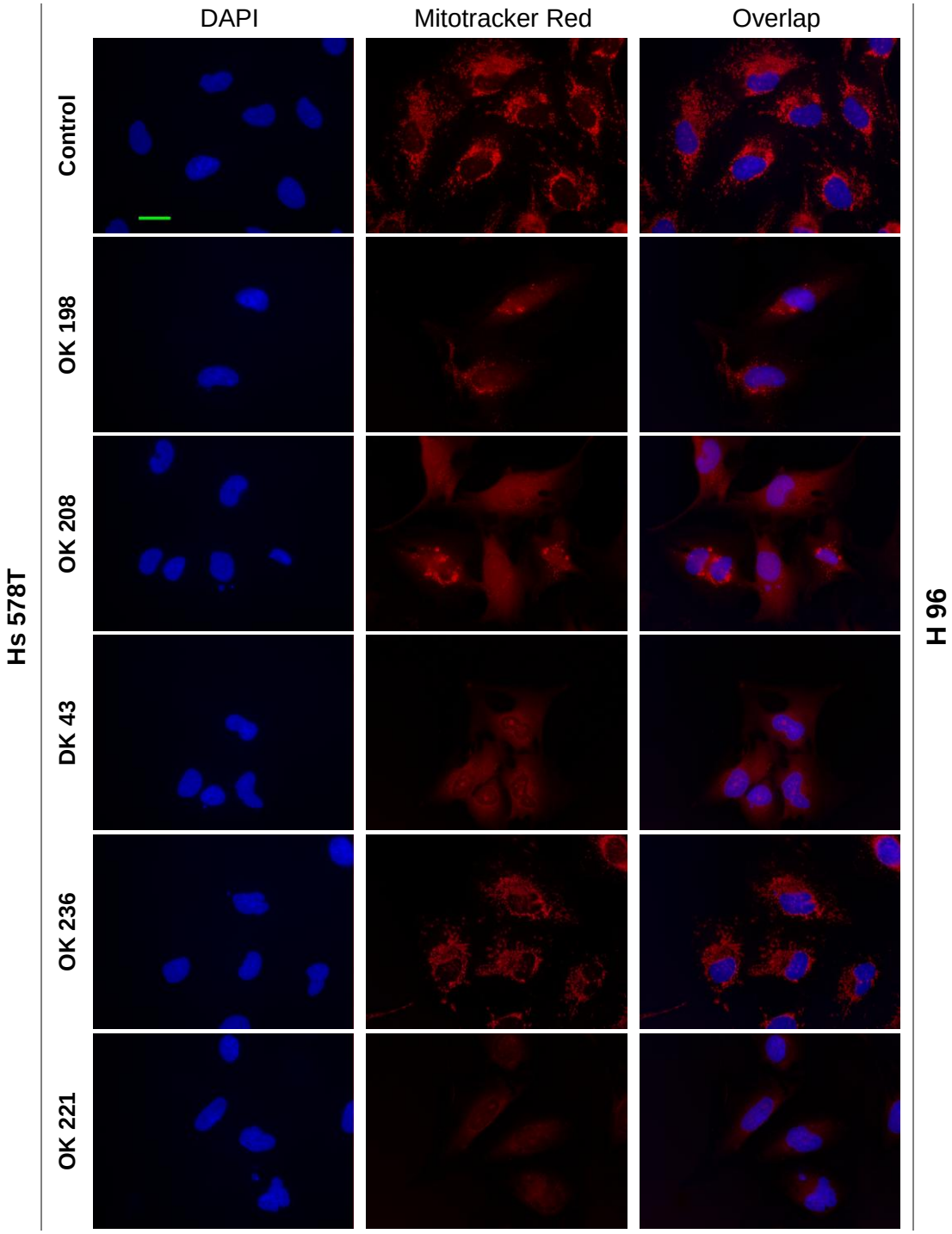

Figure 15: Epifluorescence micrographs showing the effect of DMAP triterpenoid derivatives on nuclear morphology and mitochondrial polarization in Hs 578T cell line after 96 hours of time exposure. Cells were seeded (see Materials and Methods) and incubated 24 hours later at various concentrations (**OK 221**: 0.125 µg/ml; **OK 198**: 0.5 µg/ml; **DK 43**: 1 µg/ml; **OK 208** and **OK 236**: 2 µg/ml). Thirty minutes before the end of incubation period (96 h) cells were incubated with Mitotracker Red (7.3 nM). Cells were also labeled with nuclear fluorescent dye (DAPI) prior microscope visualization. Images of DAPI and Mitotracker labeling (left and central panel, respectively) were obtained with a Zeiss Axioskop 2 Plus microscope. The right panel corresponds to an overlapping of DAPI and Mitotracker staining. The green bar represents 20µm. These results are representative of two independent experiments.

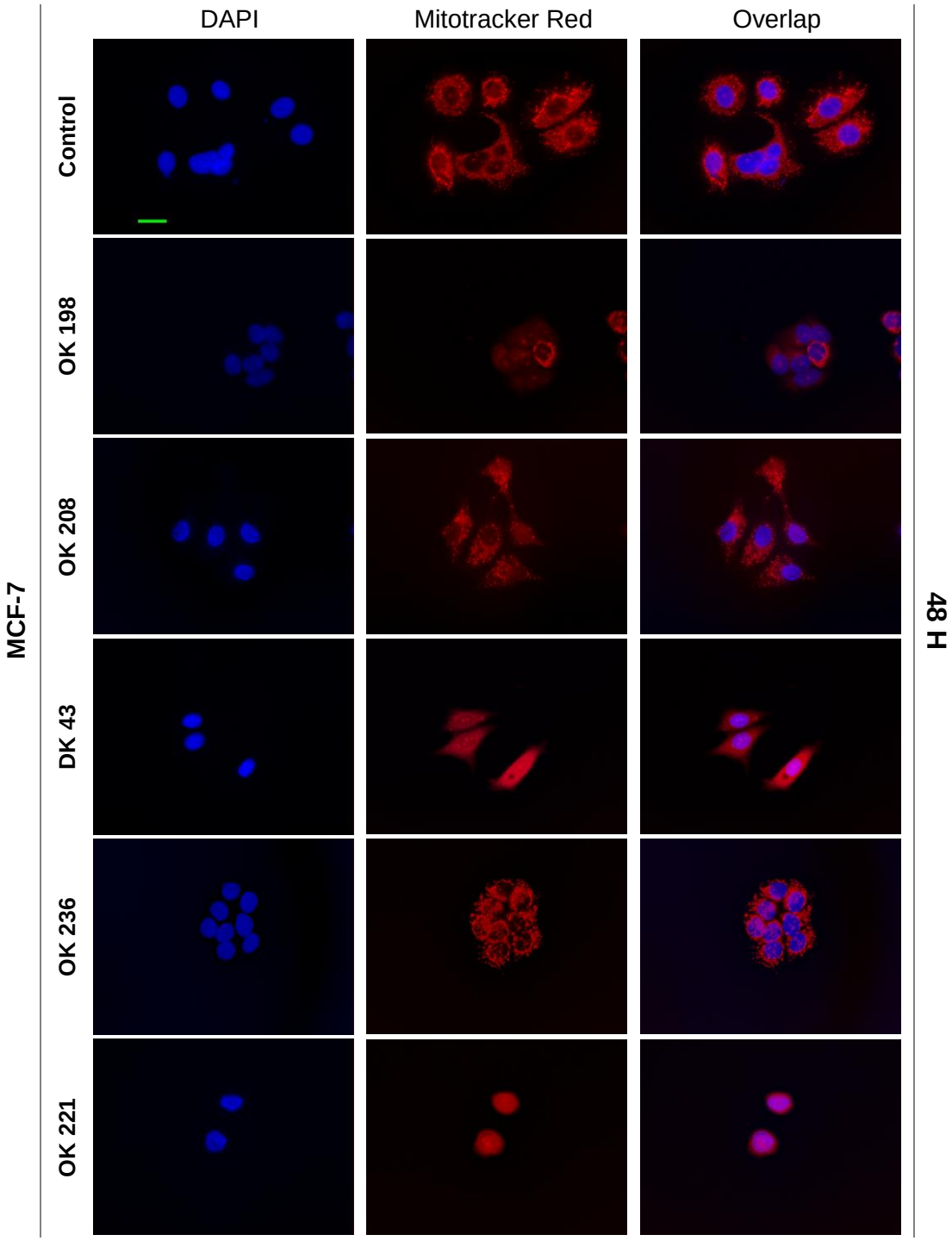

Figure 16: Epifluorescence micrographs showing the effect of DMAP triterpenoid derivatives on nuclear morphology and mitochondrial polarization in MCF-7 cell line after 48 hours of time exposure. Cells were seeded (see Materials and Methods) and incubated 24 hours later at various concentrations (**OK 221**: 0.125 µg/ml; **OK 198**: 0.5 µg/ml; **DK 43**: 1 µg/ml; **OK 208** and **OK 236**: 2 µg/ml). Thirty minutes before the end of incubation period (48 h) cells were incubated with Mitotracker Red (7.3 nM). Cells were also labeled with nuclear fluorescent dye (DAPI) prior microscope visualization. Images of DAPI and Mitotracker labeling (left and central panel, respectively) were obtained with a Zeiss Axioskop 2 Plus microscope. The right panel corresponds to an overlapping of DAPI and Mitotracker staining. The green bar represents 20µm. These results are representative of two independent experiments.

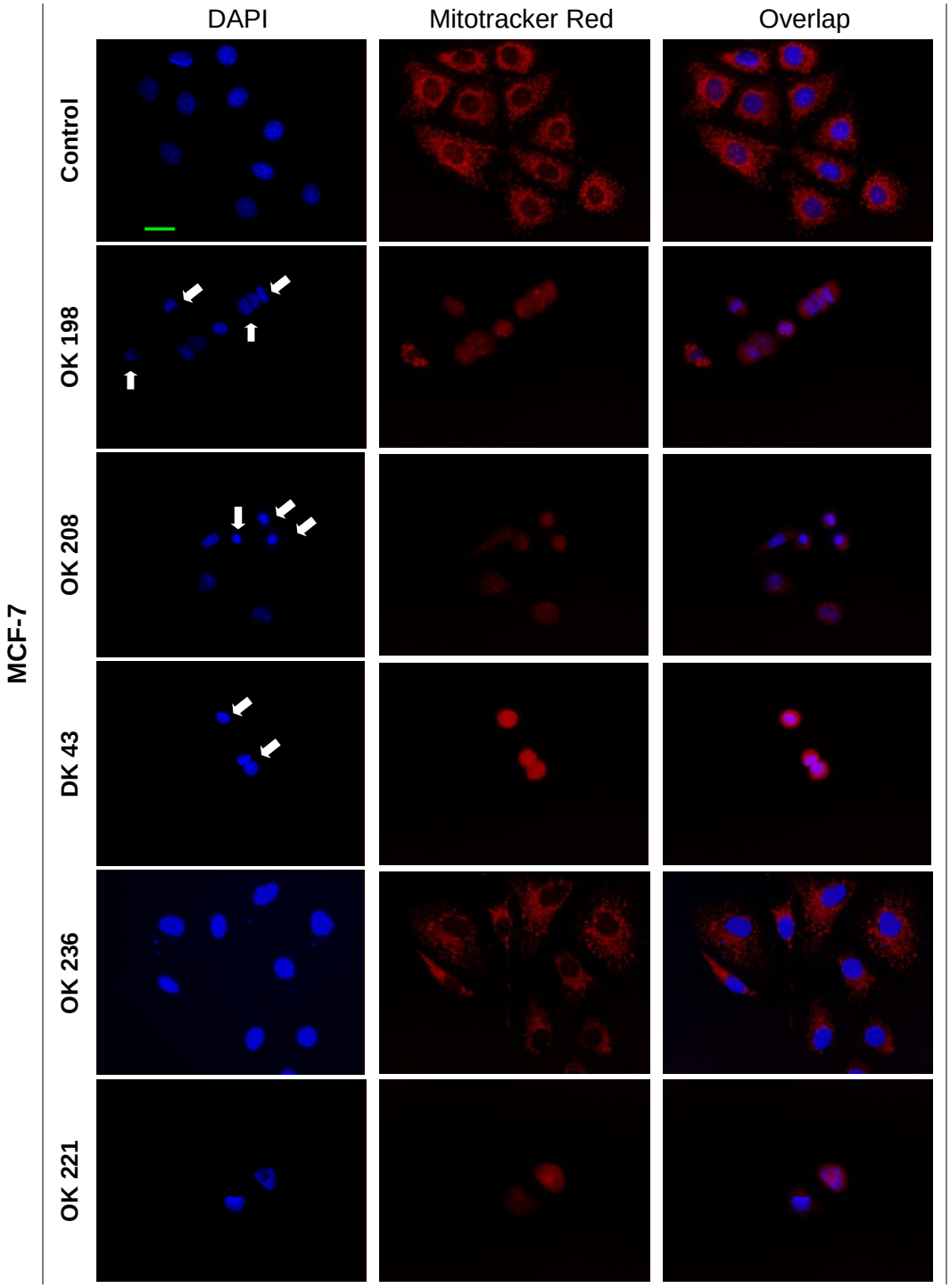

Figure 17: Epifluorescence micrographs showing the effect of DMAP triterpenoid derivatives on nuclear morphology and mitochondrial polarization in MCF-7 cell line after 96 hours of time exposure. Cells were seeded (see Materials and Methods) and incubated 24 hours later at various concentrations (**OK 221**: 0.125 µg/ml; **OK 198**: 0.5 µg/ml; **DK 43**: 1 µg/ml; **OK 208** and **OK 236**: 2 µg/ml). Thirty minutes before the end of incubation period (96 h) cells were incubated with Mitotracker (7.3 nM). Cells were also labeled with nuclear fluorescent dye (DAPI) prior microscope visualization. Images of DAPI and Mitotracker labeling (left and central panel, respectively) were obtained with a Zeiss Axioskop 2 Plus microscope. The right panel corresponds to an overlapping of DAPI and Mitotracker staining. The white arrows indicate apoptotic-like nuclei and the green bar represents 20µm. These results are representative of two independent experiments.

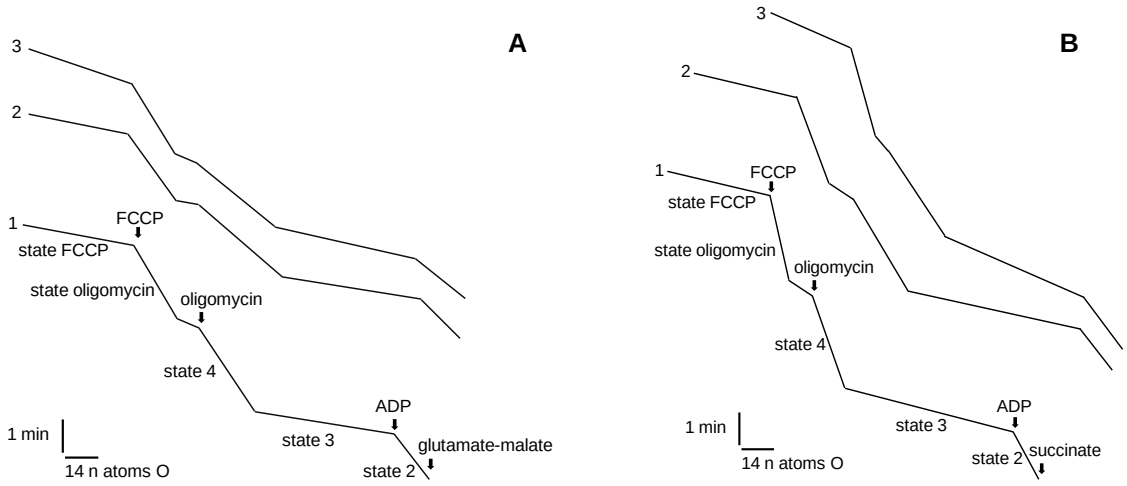

Figure 18: Typical recording of the effect of **OK 198** triterpenoid derivative on mitochondrial oxygen consumption. Hepatic mitochondria (1 mg) were incubated in 1 ml of standard respiratory medium as described in Materials and Methods. Respiration was started by adding 10 mM glutamate plus 5 mM malate (Panel A) or 5 mM succinate with 3 µM rotenone (Panel B). State 3 was initiated with 187.5 nmol of ADP. Oligomycin (1 µg) and FCCP (1 µM) were also added to the system in order to inhibit passive flux through the ATP synthase and to uncouple respiration, respectively. Line 1 corresponds to the control situation. **OK 198** 3 µg/mg protein (line 2) and 6 µg/mg protein (line 3) were preincubated with 1 mg of protein for 1 minute before the respiratory substrate.

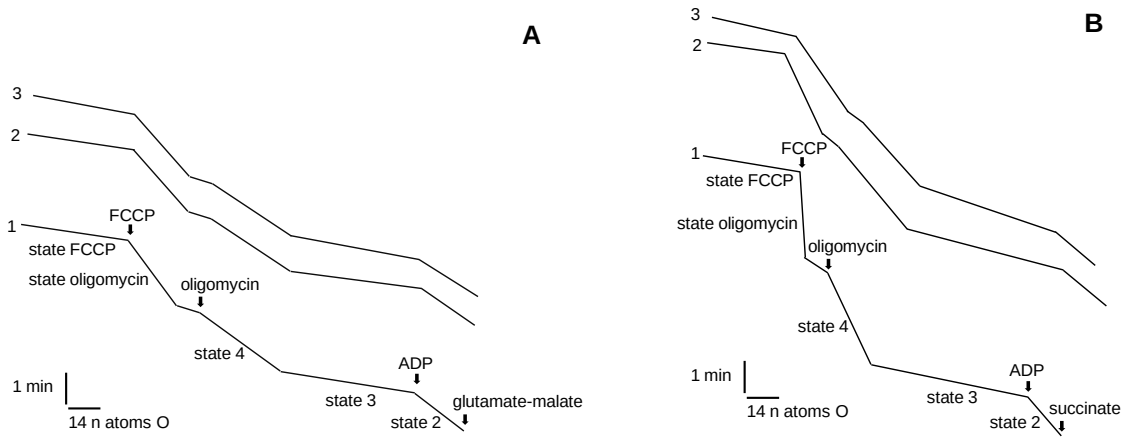

Figure 19: Typical recording of the effect of **OK 208** triterpenoid derivative on mitochondrial oxygen consumption. Hepatic mitochondria (1 mg) were incubated in 1 ml of standard respiratory medium as described in Materials and Methods. Respiration was started by adding 10 mM glutamate plus 5 mM malate (Panel A) or 5 mM succinate with 3 µM rotenone (Panel B). State 3 was initiated with 187.5 nmol of ADP. Oligomycin (1 µg) and FCCP (1 µM) were also added to the system in order to inhibit passive flux through the ATP synthase and to uncouple respiration, respectively. Line 1 corresponds to the control situation. **OK 208** 3 µg/mg protein (line 2) and 6 µg/mg protein (line 3) were preincubated with 1 mg of protein for 1 minute before the respiratory substrate.

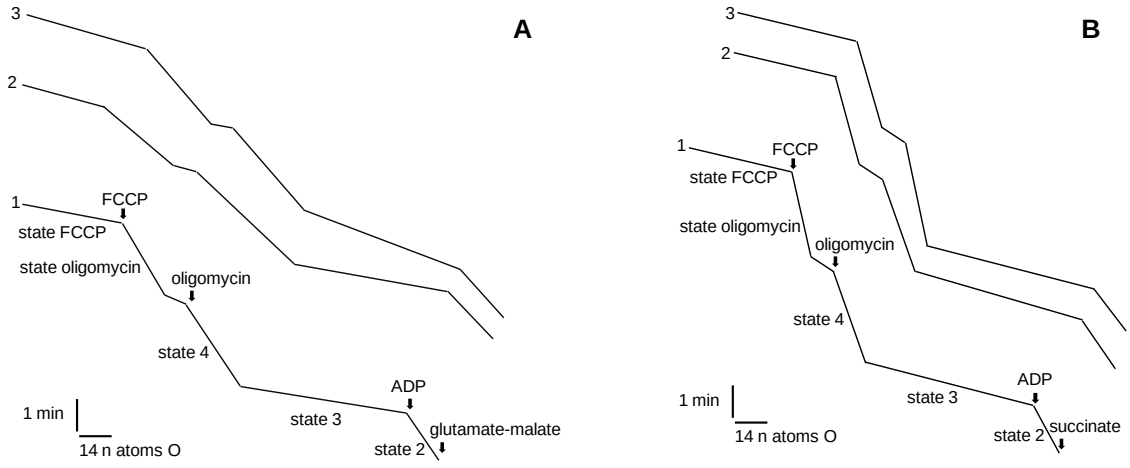

Figure 20: Typical recording of the effect of **DK 43** triterpenoid derivative on mitochondrial oxygen consumption. Hepatic mitochondria (1 mg) were incubated in 1 ml of standard respiratory medium as described in Materials and Methods. Respiration was started by adding 10 mM glutamate plus 5 mM malate (Panel A) or 5 mM succinate with 3 µM rotenone (Panel B). State 3 was initiated with 187.5 nmol of ADP. Oligomycin (1 µg) and FCCP (1µM) were also added to the system in order to inhibit passive flux through the ATP synthase and to uncouple respiration, respectively. Line 1 corresponds to the control situation. **DK 43** 3 µg/mg protein (line 2) and 6 µg/mg protein (line 3) were preincubated with 1 mg of protein for 1 minute before the respiratory substrate.

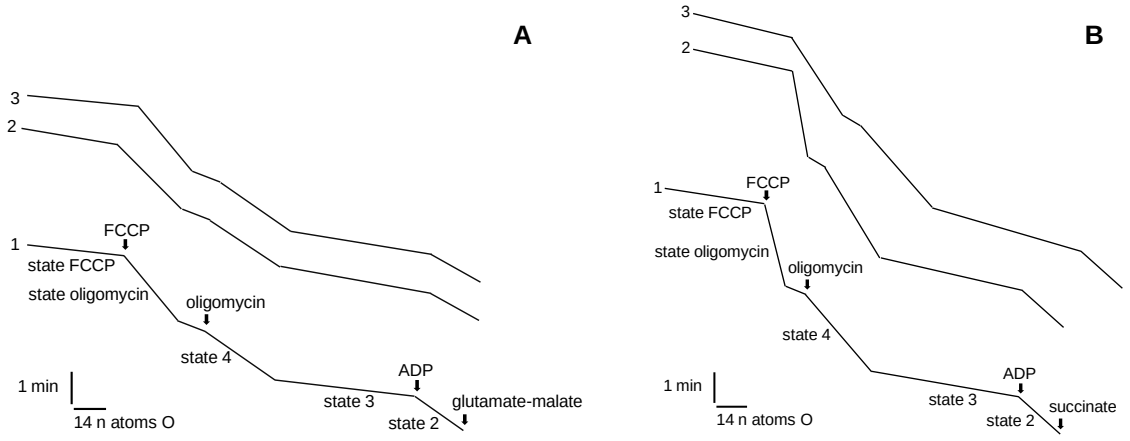

Figure 21: Typical recording of the effect of **OK 236** triterpenoid derivative on mitochondrial oxygen consumption. Hepatic mitochondria (1 mg) were incubated in 1 ml of standard respiratory medium as described in Materials and Methods. Respiration was started by adding 10 mM glutamate plus 5 mM malate (Panel A) or 5 mM succinate with 3 µM rotenone (Panel B). State 3 was initiated with 187.5 nmol of ADP. Oligomycin (1 µg) and FCCP (1 µM) were also added to the system in order to inhibit passive flux through the ATP synthase and to uncouple respiration, respectively. Line 1 corresponds to the control situation. **OK 236** 3 µg/mg protein (line 2) and 6 µg/mg protein (line 3) were preincubated with 1 mg of protein for 1 minute before the respiratory substrate.

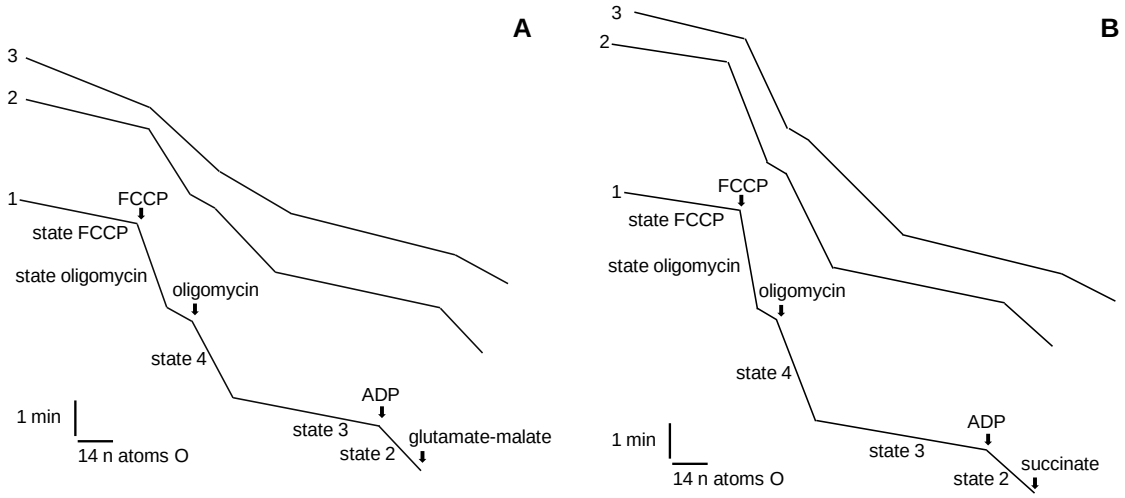

Figure 22: Typical recording of the effect of **OK 221** triterpenoid derivative on mitochondrial oxygen consumption. Hepatic mitochondria (1 mg) were incubated in 1 ml of standard respiratory medium as described in Materials and Methods. Respiration was started by adding 10 mM glutamate plus 5 mM malate (Panel A) or 5 mM succinate with 3 µM rotenone (Panel B). State 3 was initiated with 187.5 nmol of ADP. Oligomycin (1 µg) and FCCP (1µM) were also added to the system in order to inhibit passive flux through the ATP synthase and to uncouple respiration, respectively. Line 1 corresponds to the control situation. **OK 221** 3 µg/mg protein (line 2) and 6 µg/mg protein (line 3) were preincubated with 1 mg of protein for 1 minute before the respiratory substrate.

3.4 DMAP Triterpenoid Derivatives Effects on Isolated Hepatic Mitochondria: Evaluation of the $\Delta\psi_m$ Fluctuations

To investigate the effect of triterpenoid derivatives on mitochondrial $\Delta\psi$ generation, both glutamate/malate (substrate for complex I) and succinate (substrate for complex II) were used as substrates. The same range of concentrations used in mitochondrial respiratory parameters was used for this assay (3 and 6 µg/mg of protein). A typical recording of the effect of each one of the tested compounds on mitochondrial transmembrane electric potential are represented in figures 24 to 28. The results for maximum $\Delta\psi_m$, compound-induced depolarization, and phosphorylative lag phase are described in tables 1 to 5. The generation of mitochondrial transmembrane electric potential shows a slight increase (for increasing concentrations) when compared to the control for **OK 198** triterpenoid derivative due to its interference with ATP synthase Fo subunit (Table 1). For the remaining compounds, there appears to be a trend for a depolarization decrease and lag phase increase for increasing concentrations of the tested compounds for both glutamate/malate or succinate

energized mitochondria. The increase of the lag phase can be partly explained by the induced depolarization of the compound itself due to its positive charge nature. However, the depolarization induced by **OK 221** is also notoriously linked to direct effects on the respiratory chain and to the enhanced permeabilization to protons (Figure 23).

3.5 DMAP Triterpenoid Derivatives Stimulate the MPT on Isolated Hepatic Mitochondria

The irreversible form of MPT pore opening is accompanied by an increase in mitochondrial internal volume (mitochondrial swelling) and by a decrease in mitochondrial transmembrane electric potential. The two phenomena can be followed experimentally by measuring the changes in the suspension absorbance at 540 nm and using a TTP^+ selective electrode, respectively. The MPT pore opening was induced by Ca^{2+} in a phosphate-buffer medium and measured in the presence and absence of increasing concentrations of DMAP triterpenoid derivatives. Figure 30 shows a typical recording of the effect of the tested compounds on calcium-induced MPT pore opening followed by measuring $\Delta\psi_m$ fluctuations. Increasing concentrations of **DK 43** and **OK 236** have cause calcium-induced Δψm dissipation, with **OK 198**, **OK 208** and **OK 221** having the more pronounced effect. An additional control with FCCP was performed in order to investigate if the MPT pore induction was due to a small decrease in $\Delta\psi_m$, which did not happen. Similarly to what happened in $\Delta\psi_m$ fluctuations, mitochondrial swelling was most drastically observed for increasing concentrations of **OK 198**, **OK 208** and **OK 221**, with **DK 43** and **OK 236** having the lower effects for the chosen concentrations (figure 29, Panel A and B). Both approaches denote that the effect of tested compounds in MPT pore induction is dose-dependent. The permeability transition pore inhibitor [72], cyclosporin A, was able to prevent both mitochondrial swelling and $\Delta\psi_m$ dissipation, confirming that this effect is caused by MPT pore induction.

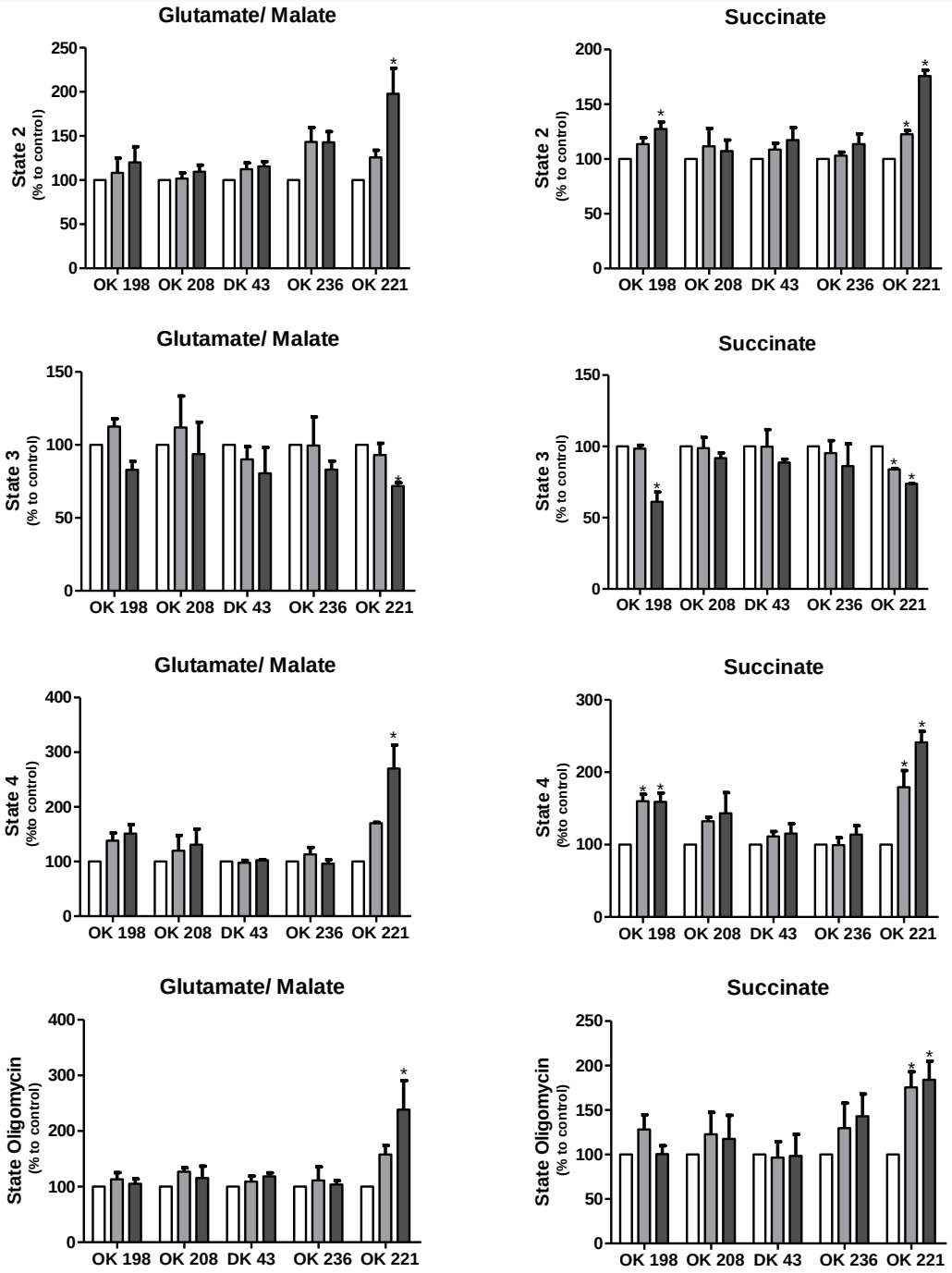
Glutamate/ Malate
State 2 (% to control)
250
200
150
100
50
0
OK 198 OK 208 DK 43 OK 236 OK 221
Succinate
State 2 (% to control)
200
150
100
50
0
OK 198 OK 208 DK 43 OK 236 OK 221
Glutamate/ Malate
State 3 (% to control)
150
100
50
0
OK 198 OK 208 DK 43 OK 236 OK 221
Succinate
State 3 (% to control)
150
100
50
0
OK 198 OK 208 DK 43 OK 236 OK 221
Glutamate/ Malate
State 4 (%to control)
400
300
200
100
0
OK 198 OK 208 DK 43 OK 236 OK 221
Succinate
State 4 (%to control)
300
200
100
0
OK 198 OK 208 DK 43 OK 236 OK 221
Glutamate/ Malate
State Oligomycin (% to control)
400
300
200
100
0
OK 198 OK 208 DK 43 OK 236 OK 221
Succinate
State Oligomycin (% to control)
250
200
150
100
50
0
OK 198 OK 208 DK 43 OK 236 OK 221

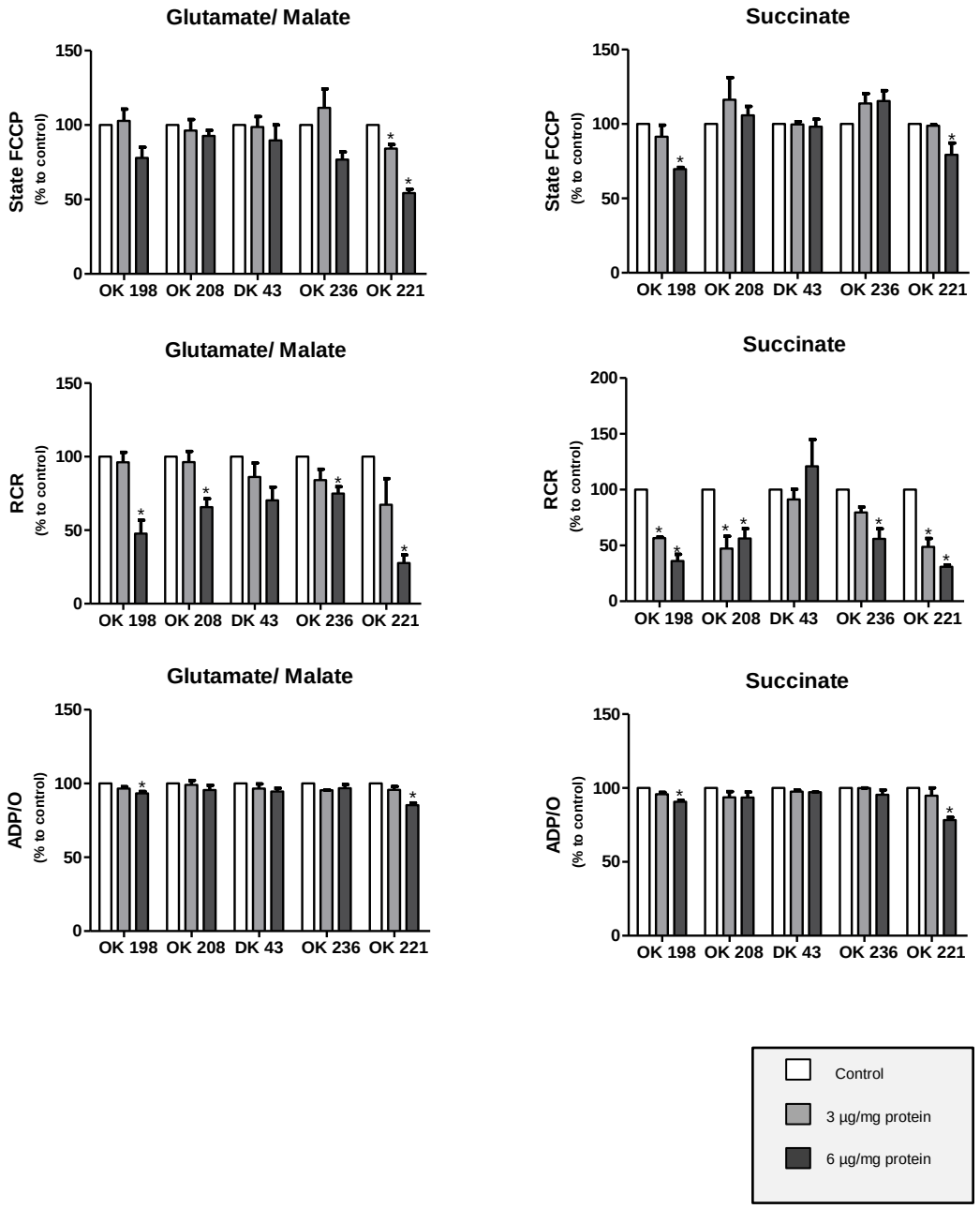

Figure 23: Effects of triterpenoid derivatives on mitochondrial respiraty parameters energized with 10 mM glutamate/ 5 mM malate (left panel) or 5 mM succinate (right panel). Mitochondria were incubated in 1ml respiration medium (see Materials and Methods section). ADP (187.5 nmol) was added to induce state 3 respiration. Oligomycin (1 µg) and FCCP (1 µM) were added to the system in order to inhibit passive flux through ATP synthase and to uncouple respiration, respectively. The RCR was calculated as the ratio between sate 3 and sate 4 respiration. The ADP/O ratio was calculated as the number of nmol ADP phosphorylated by natoms of O consumed during ADP phosphorylation. Data were expressed as % to control and are means ± SEM of tree different preparations. * $p < 0.05$ vs. control. Control values for Complex I: State 2 = 19.0 ± 4.1 natoms O/min / mg protein; State 3 = 124.1 ± 20.2 natoms O/min / mg protein; State 4 = 18.0 ± 5.2 natoms O/min / mg protein; State Oligomycin = 9.3 ± 2.9 natoms O/min / mg protein; ADP/O = 2.9 ± 0.1; RCR = 9.3 ± 2.0 (Mean ± SEM, n=3). Control values for Complex II: State 2 = 22.3 ± 5.5 natoms O/min / mg protein; State 3 = 131.8 ± 8.5 natoms O/min / mg protein; State 4 = 18.3 ± 3.3 natoms O/min / mg protein; State Oligomycin= 8.3 ± 2.5; natoms O/min / mg protein; State FCCP = 158.2 ± 25.2; ADP/O = 2.0 ± 0.2; RCR = 6.6 ± 2.1(Means ± SEM, n=3).

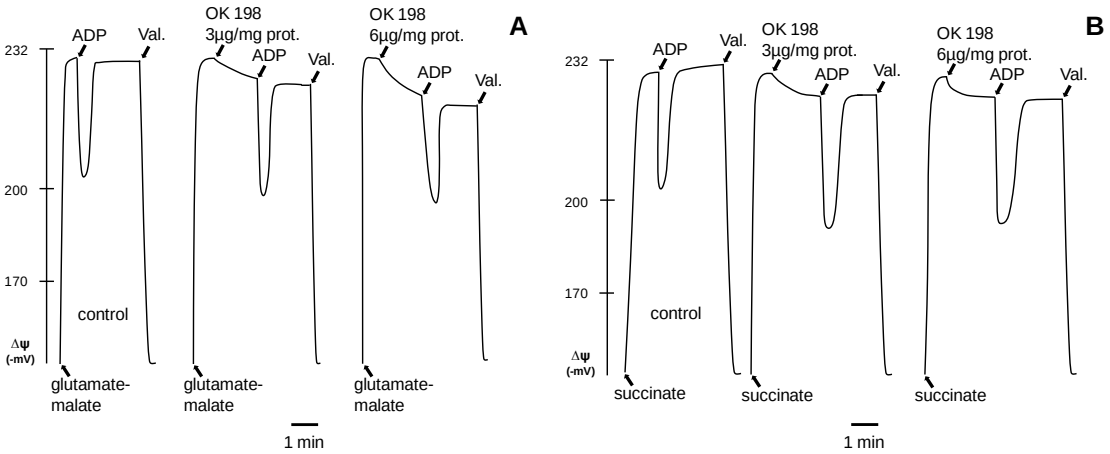

Figure 24: Representative recording of the effect of **OK 198** triterpenoid derivative on mitochondrial transmembrane electric potential. Hepatic mitochondria (1 mg) were incubated in 1 ml of standard reaction medium as described in Materials and Methods. Mitochondria were energized by adding 5 mM glutamate/2.5 mM malate (Panel A) or 5 mM succinate with 3 µM rotenone (Panel B). ADP (125 nmol) was added to initiate state 3 and valinomycin (Val.) 0.2 µg was added to the system in order to confirm if **OK 198** interferes with the TPP^+ electrode. **OK 198** 3 µg/mg protein and 6 µg/mg protein were preincubated with 1 mg of protein for 1 minute prior the ADP addition.

Table 1: Effect of **OK 198** on glutamate-malate (for complex I) and succinate (substrate for complex II) energized mitochondria. $\Delta\psi_m$ Max., compound depolarization, ADP depolarization and lag phase were measured indirectly, using a TTP^+ selective electrode (see Materials and Methods section). Data are means ±SEM of tree independent preparations. * $p < 0.05$ vs. control. Parenthesis values represent % to control. n.m. = not measurable.

	$\Delta\psi_m$ max. (-mV)	**Compound depolarization (-mV)**	**ADP depolarization (-mV)**	**Lag phase (sec)**
Complex I				
Control	223.8 ± 7.5 (100%)	n.m.	20.2 ± 5.5 (100%)	32.8 ± 8.8 (100%)
3 µg/mg	224.8 ± 7.0 (100.4% ± 0.3)	4.6 ± 0.7	22.5 ± 4.9 (112.3% ± 7.8)	28.8 ± 3.8 (90.0% ± 13.5)
6 µg/mg	224.6 ± 7.3 (100.3% ± 0.2)	5.7 ± 1.4	22.6 ± 4.9 (112.9% ± 7.4)	31.0 ± 8.5 (94.4% ± 5.6)
Complex II				
Control	225.4 ± 4.1 (100%)	n.m.	26.7 ± 5.5 (100%)	37.0 ± 3.6 (100%)
3 µg/mg	225.6 ± 4.6 (100.1% ± 0.9)	3.0 ± 1.3	28.5 ± 6.9 (106.1% ± 10.4)	39.0 ± 5.2 (105.2% ± 5.3)
6 µg/mg	224.4 ± 5.8 (99.6% ± 1.2)	3.5 ± 1.1	27.8 ± 6.6 (104.2% ± 16.0)	42.0 ± 6.0 (113.2% ± 5.9)

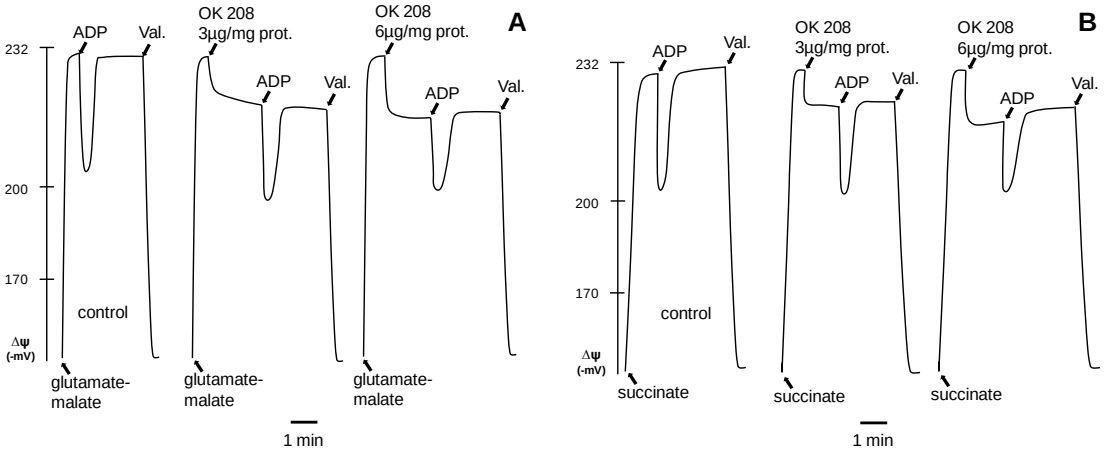

Figure 25: Representative recording of the effect of **OK 208** triterpenoid derivative on mitochondrial transmembrane electric potential. Hepatic mitochondria (1 mg) were incubated in 1 ml of standard reaction medium as described in Materials and Methods. Mitochondria were energized by adding 5 mM glutamate/2.5 mM malate (Panel A) or 5 mM succinate with 3 µM rotenone (Panel B). ADP (125 nmol) was added to initiate state 3 and valinomycin (Val.) 0.2 µg was added to the system in order to confirm if **OK 208** interferes with the TPP^+ electrode. **OK 208** 3 µg/mg protein and 6 µg/mg protein were preincubated with 1 mg of protein for 1 minute prior the ADP addition.

Table 2: Effect of **OK 208** on glutamate-malate (for complex I) and succinate (substrate for complex II) energized mitochondria. $\Delta\psi_m$ Max., compound depolarization, ADP depolarization and lag phase were measured indirectly, using a TTP^+ selective electrode (see Materials and Methods section). Data are means ±SEM of tree independent preparations. * $p < 0.05$ vs. control. Parenthesis values represent % to control. n.m. = not measurable.

	$\Delta\psi_m$ max. (-mV)	**Compound depolarization (-mV)**	**ADP depolarization (-mV)**	**Lag phase (sec)**
Complex I				
Control	223.8 ± 7.5 (100%)	n.m.	20.2 ± 5.5 (100%)	35.8 ± 10.3 (100%)
3 µg/mg	224.8 ± 8.0 (100.4% ± 0.8)	10.9 ± 2.6	18.5 ± 3.4 (94.2% ± 17.9)	42.8 ± 7.4 (121.6% ± 14.1)
6 µg/mg	225.8 ± 5.4 (100.9% ± 1.1)	16.3 ± 3.7	14.6 ± 3.1 (73.9% ± 13.8)	46.5 ± 19.1 (127.7% ± 16.8)
Complex II				
Control	230.9 ± 12.2 (100%)	n.m.	33.6 ± 7.9 (100%)	31.0 ± 5.7 (100%)
3 µg/mg	231.8 ± 11.7 (100.4% ± 0.3)	10.5 ± 2.7	30.3 ± 7.0 (90.2% ± 3.3)	36.0 ± 7.6 (116.8% ± 2.9)
6 µg/mg	228.3 ± 8.7 (99.0% ± 1.6)	15.4 ± 3.5	27.8 ± 7.2 (82.7% ± 7.0) *	45.5 ± 3.5 (148.2% ± 15.6) *

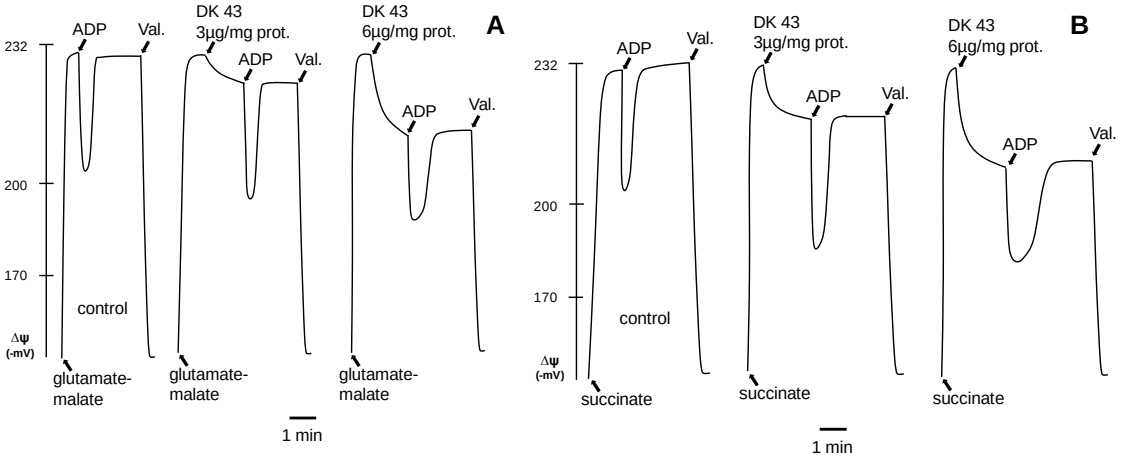

Figure 26: Representative recording of the effect of **DK 43** triterpenoid derivative on mitochondrial transmembrane electric potential. Hepatic mitochondria (1 mg) were incubated in 1 ml of standard reaction medium as described in Materials and Methods. Mitochondria were energized by adding 5 mM glutamate/2.5 mM malate (Panel A) or 5 mM succinate with 3 µM rotenone (Panel B). ADP (125 nmol) was added to initiate state 3 and valinomycin (Val.) 0.2 µg was added to the system in order to confirm if **DK 43** interferes with the TPP^+ electrode. **DK 43** 3 µg/mg protein and 6 µg/mg protein were preincubated with 1 mg of protein for 1 minute prior the ADP addition.

Table 3: Effect of **DK 43** on glutamate-malate (for complex I) and succinate (for complex II) energized mitochondria. $\Delta\psi_m$ Max., compound depolarization, ADP depolarization and lag phase were measured indirectly, using a TTP^+ selective electrode (see Materials and Methods section). Data are means ±SEM of tree independent preparations. * $p < 0.05$ vs. control. Parenthesis values represent % to control. n.m. = not measurable.

	$\Delta\psi_m$ max. (-mV)	**Compound depolarization (-mV)**	**ADP depolarization (-mV)**	**Lag phase (sec)**
Complex I				
Control	221.4 ± 3.9 (100%)	n.m.	23.0 ± 1.9 (100%)	27.8 ± 1.1 (100%)
3 µg/mg	222.0 ± 1.2 (100.3% ± 1.3)	7.3 ± 1.3	26.5 ± 2.1 (115.0% ± 5.1)	27.8 ± 3.2 (100.3% ± 15.3)
6 µg/mg	221.6 ± 1.7 (100.1% ± 1.7)	15.7 ± 3.6	23.5 ± 3.2 (102.8% ± 19.6)	45.0 ± 8.5 (162.9% ± 36.8)
Complex II				
Control	230.9 ± 12.2 (100%)	n.m.	33.6 ± 7.9 (100%)	33.3 ± 6.5 (100%)
3 µg/mg	232.3 ± 13.0 (100.6% ± 0.3)	10.6 ± 6.4	36.2 ± 3.2 (110.7% ± 18.8)	38.0 ± 1.7 (116.3% ± 18.0)
6 µg/mg	227.8 ± 14.0 (98.7% ± 2.1)	16.6 ± 9.2	29.9 ± 4.4 (92.8% ± 29.7)	53.0 ± 7.5 * (164.8% ± 46.2) *

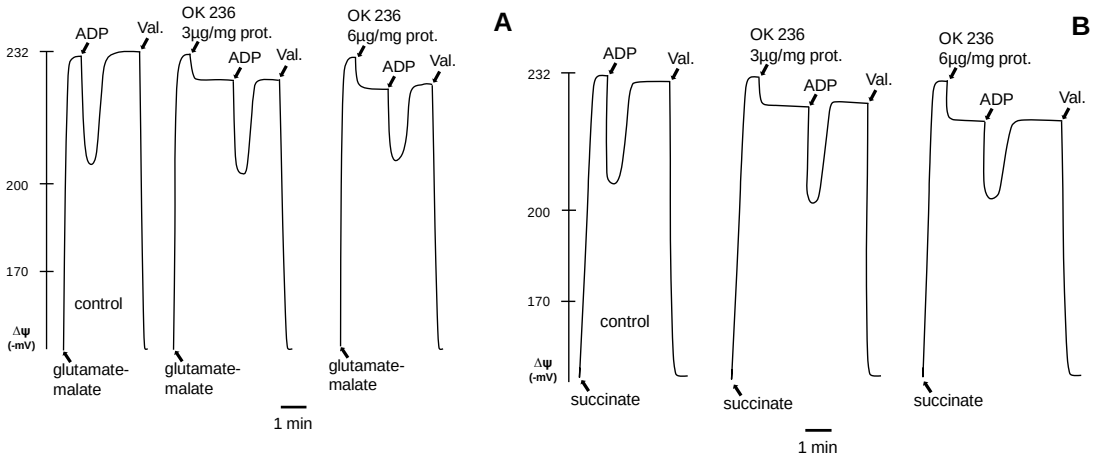

Figure 27: Representative recording of the effect of **OK 236** triterpenoid derivative on mitochondrial transmembrane electric potential. Hepatic mitochondria (1 mg) were incubated in 1 ml of standard reaction medium as described in Materials and Methods. Mitochondria were energized by adding 5 mM glutamate/2.5 mM malate (Panel A) or 5 mM succinate with 3 µM rotenone (Panel B). ADP (125 nmol) was added to initiate state 3 and valinomycin (Val.) 0.2 µg was added to the system in order to confirm if **OK 236** interferes with the TPP^+ electrode. **OK 236** 3 µg/mg protein and 6 µg/mg protein were preincubated with 1 mg of protein for 1 minute prior the ADP addition.

Table 4: Effect of **OK 236** on glutamate-malate (for complex I) and succinate (for complex II) energized mitochondria. $\Delta\psi_m$ Max., compound depolarization, ADP depolarization and lag phase were measured indirectly, using a TTP^+ selective electrode (see Materials and Methods section). Data are means ±SEM of tree independent preparations. The results were not statistically different (treatments vs. control) for a p value < 0.05. Parenthesis values represent % to control. n.m. = not measurable.

	$\Delta\psi_m$ max. (-mV)	**Compound depolarization (-mV)**	**ADP depolarization (-mV)**	**Lag phase (sec)**
Complex I				
Control	224.8 ± 10.9 (100%)	n.m.	25.3 ± 5.6 (100%)	36.5 ± 9.2 (100%)
3 µg/mg	225.3 ± 12.5 (100.2% ± 0.7)	6.2 ± 0.1	23.4 ± 2.8 (93.6% ± 9.3)	36.8 ± 5.3 (102.1% ± 11.2)
6 µg/mg	225.3 ± 13.3 (100.2% ± 1.1)	10.2 ± 3.9	20.3 ± 1.2 (81.8% ± 13.2)	46.0 ± 1.4 (129.7% ± 28.8)
Complex II				
Control	232.5 ± 16.8 (100%)	n.m.	36.1 ± 8.2 (100%)	36.5 ± 4.9 (100%)
3 µg/mg	231.7 ± 15.7 (99.7% ± 0.5)	6.2 ± 0.4	30.6 ± 3.4 (85.8% ± 9.9)	38.3 ± 9.5 (104.0% ± 12.1)
6 µg/mg	229.2 ± 14.7 (98.6% ± 0.8)	8.3 ± 0.6	27.7 ± 3.9 (79.9% ± 29.0)	40.0 ± 4.2 (109.8% ± 3.3)

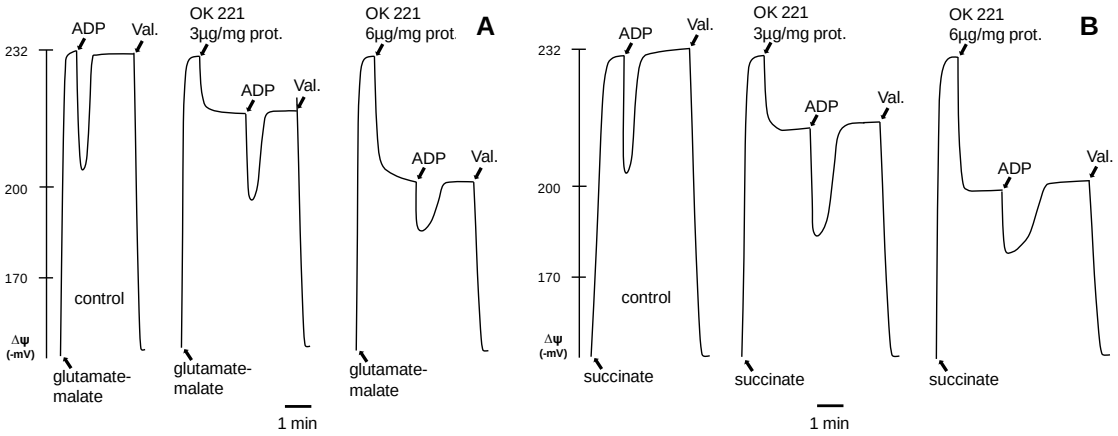

Figure 28: Representative recording of the effect of **OK 221** triterpenoid derivative on mitochondrial transmembrane electric potential. Hepatic mitochondria (1 mg) were incubated in 1 ml of standard reaction medium as described in Materials and Methods. Mitochondria were energized by adding 5 mM glutamate/2.5 mM malate (Panel A) or 5 mM succinate with 3 µM rotenone (Panel B). ADP (125 nmol) was added to initiate state 3 and valinomycin (Val.) 0.2 µg was added to the system in order to confirm if **OK 221** interferes with the TPP^+ electrode. **OK 221** 3 µg/mg protein and 6 µg/mg protein were preincubated with 1 mg of protein for 1 minute prior the ADP addition.

Table 5: Effect of **OK 221** on glutamate-malate (for complex I) and succinate (for complex II) energized mitochondria. $\Delta\psi_m$ Max., compound depolarization, ADP depolarization and lag phase were measured indirectly, using a TTP^+ selective electrode (see Materials and Methods section). Data are means ±SEM of tree independent preparations. * $p < 0.05$ vs. control. Parenthesis values represent % to control. n.m. = not measurable.

	$\Delta\psi_m$ max. (-mV)	**Compound depolarization (-mV)**	**ADP depolarization (-mV)**	**Lag phase (sec)**
Complex I				
Control	228.8 ± 5.5 (100%)	n.m.	17.9 ± 6.3 (100%)	33.5 ± 4.3 (100%)
3 µg/mg	228.7 ± 7.0 (100.0% ± 0.7)	12.0 ± 2.6	19.5 ± 4.0 (112.1% ± 15.9)	51.0 ± 7.9 * (151.9% ± 5.7) *
6 µg/mg	229.2 ± 4.9 (100.2% ± 0.3)	22.3 ± 6.9	13.5 ± 1.1 (79.5% ± 18.1)	63.3 ± 4.5 * (190.3% ± 16.1) *
Complex II				
Control	227.9 ± 0.3 (100%)	n.m.	25.1 ± 6.4 (100%)	43.0 ± 8.7 (100%)
3 µg/mg	228.1 ± 1.5 (100.1% ± 0.8)	13.8 ± 1.6	22.4 ± 6.0 (88.9% ± 7.0)	40.3 ± 8.1 (96.3% ± 25.2)
6 µg/mg	227.7 ± 2.7 (99.9% ± 1.3)	24.8 ± 5.6	13.8 ± 4.7 (54.6% ± 11.3) *	57.0 ± 3.0 (137.7% ± 38.3)

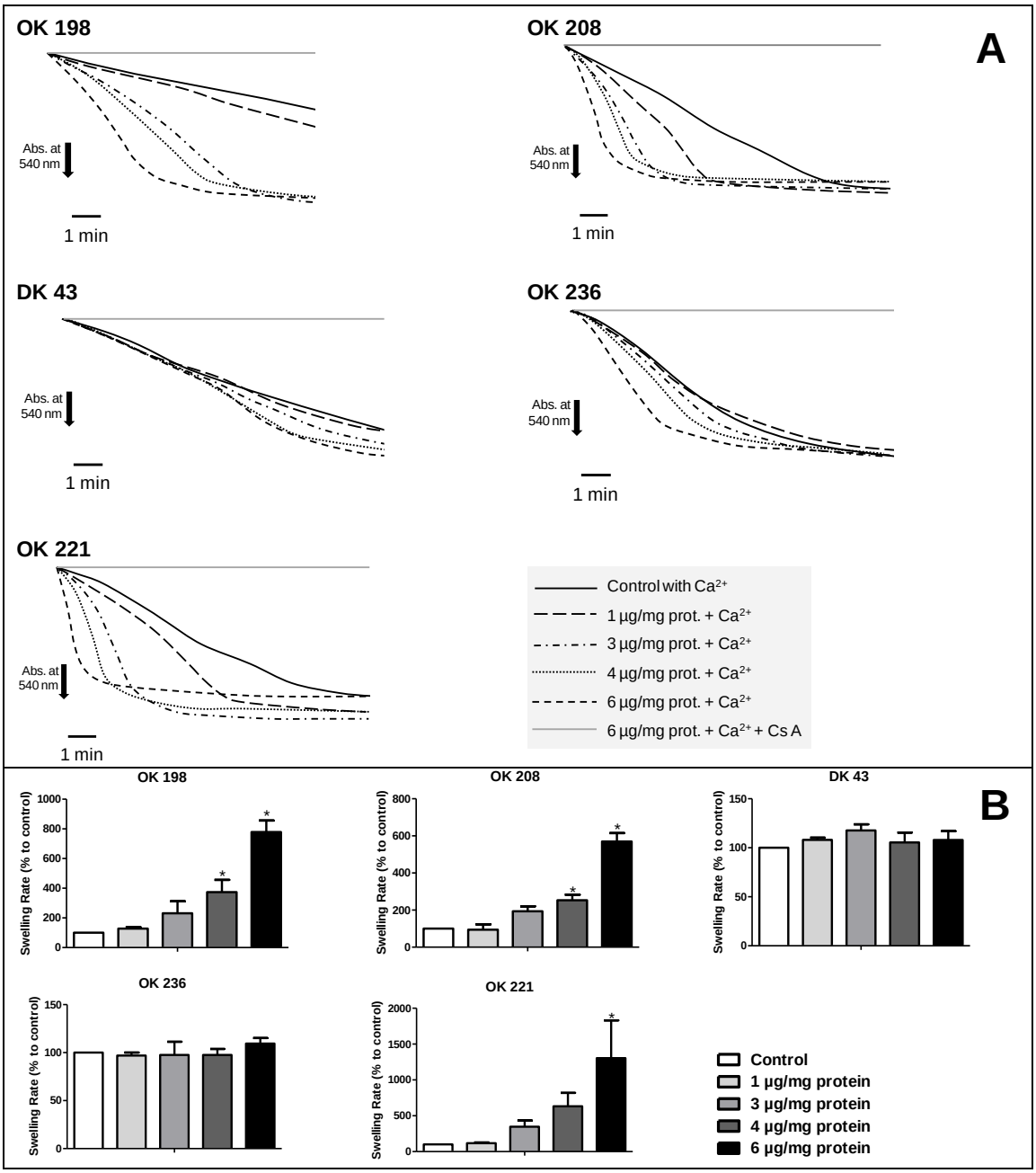

Figure 29: Typical recording of the effect of increasing concentrations of triterpenoid derivatives on calcium-induced MPT pore followed by measuring variations in mitochondrial volume and evaluated by the decrease of optical density at 540nm (Panel A). Hepatic mitochondria (1 mg) were suspended in 2 ml of swelling medium and energized by succinate (5 mM) as described in Material and Methods section. Triterpenoid derivatives at various concentrations were allowed to incubate with mitochondria. Calcium (depending on the mitochondrial preparation) was added to the system in order to induce MPT pore. For each assay, a negative control with cyclosporin A was performed in order to prevent mitochondrial swelling. Cs A was preincubated with mitochondrial suspension before the addition of tested compounds (at maximum concentrations) and calcium. Panel B represents the triterpenoid derivatives effect on Ca^{2+}-induced mitochondrial swelling evaluated by the decrease of optical density at 540nm. Data are means ± SEM of three to four independent preparations. * $p < 0.05$ vs. control. Values are expressed as % to the control.

OK 198

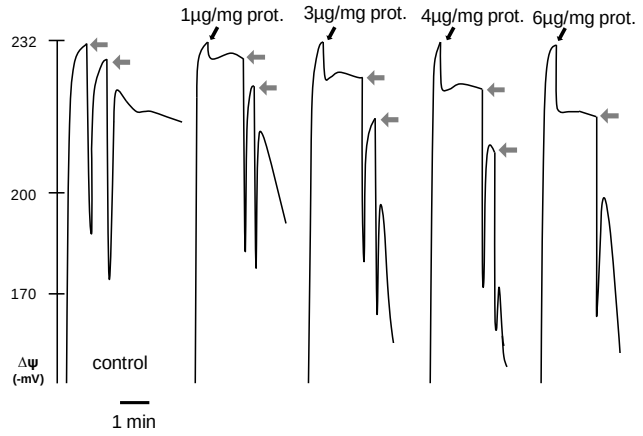

OK 208

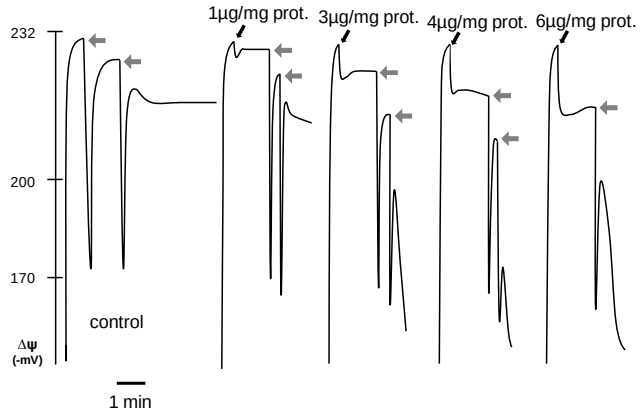

DK 43

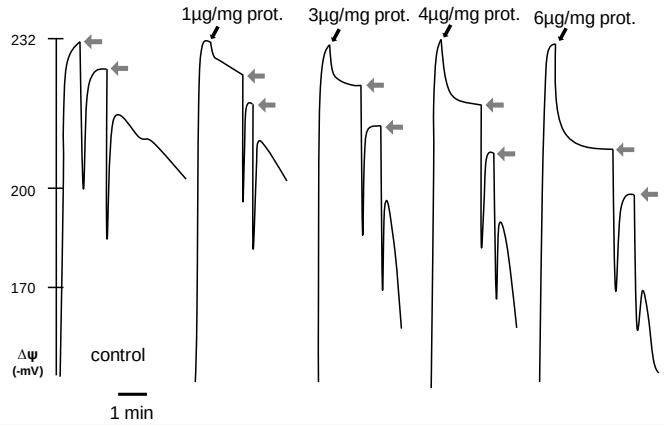

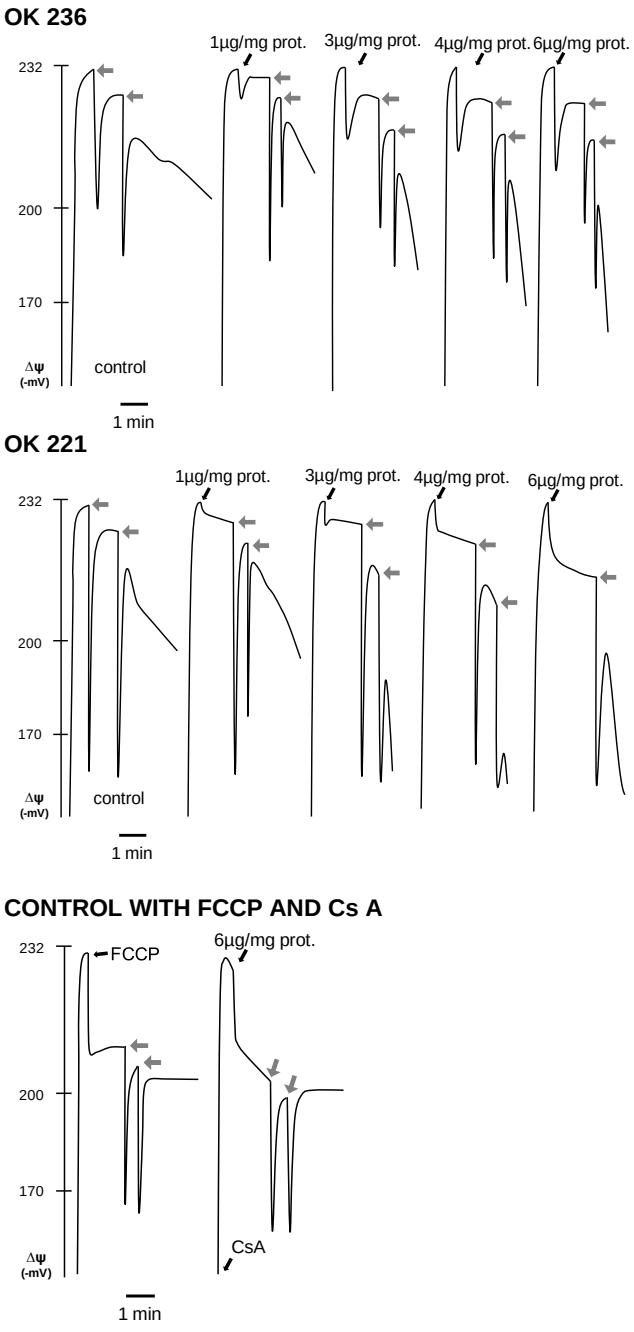

Figure 30: Representative recording of the effect of increasing concentrations of triterpenoid derivatives on calcium-induced MPT pore indirectly followed by measuring $\Delta\psi_m$ fluctuations, using a TTP^+ selective electrode (see Materials and Methods). Mitochondria were incubated in 1 ml of swelling medium and energized by succinate (5 mM). Triterpenoid derivatives at various concentrations were incubated for 2 minutes with mitochondria. Calcium (depending on the mitochondrial preparation) was added to the system in order to induce MPT pore. Control with FCCP was performed in order to verify if MPT pore was induced due to the decrease of $\Delta\psi_m$. Control with Cs A was carried out for **OK 198** and for other compounds (data not shown) in order to prevent mitochondrial swelling. Cs A was preincubated with mitochondrial suspension before the addition of tested compounds (highest concentrations) and calcium. Calcium additions are represented by grey arrows.

Discussion

CHAPTER

4

The increased resistance to apoptosis induction is a common feature in cancers. Since mitochondria occupy a strategic position between bioenergetic/biosynthetic metabolism and cell death regulation, these organelles emerged as idealized targets for cancer therapy. Thus, compounds that directly affect mitochondrial functions and trigger apoptosis are considered as very promising anti-cancer agents. Triterpenoids are a class of natural occurring compounds with ubiquitous distribution and whose anticancer activity was already documented and observed to be dependent on apoptosis induction via direct mitochondrial alterations. Betulinic acid is one of such natural compounds that display notable level of discrimination in promoting apoptosis in some cancer cell lines such as melanoma [61], glioma and ovarian carcinoma [60]. Although extracted from flora in large amounts, the use of these triterpenoids as it stands in nature remains quite limited. In this way, taking advantage of quantitative structure-activity relationships (QSARs), derivatives of triterpenoids can be synthesized in order to produce more active and selective compounds. With this in mind, dimethylaminopyridine (DMAP) derivatives of lupane triterpenoids were synthesized based on birch bark lupane triterpenoids betulin and betulinic acid, and are under consideration for their potent effect on cancer cell lines [60].

Our research group has previously tested a number of DMAP derivatives on human melanoma cell lines [56]. These compounds induced mitochondrial fragmentation and depolarization, along with an inhibition of cell proliferation. The potency of their effects was correlated with the number, position, and orientation of the DMAP groups. Overall, the extent of proliferation inhibition was shown to mirror the effectiveness of mitochondrial disruption.

The present work is a logical sequence to the initial results, aiming at understanding in more detail the mechanisms behind the mitochondrial toxicity observed in the previous study, trying at the same time to correlate those same effects with a possible selective anti-cancer activity. The latter was here also tested by performing proliferation assays on two human breast cancer cell lines vs. one non-tumor cell line.

All the DMAP triterpenoid derivatives in study have a hydrophobic central region composed by four cyclohexane rings and one cyclopentane ring which corresponds to betulinic acid. Polar groups were added to the structure backbone in order to provide an amphiphilic character to molecules. This anellar-like structure gives a planar geometry to molecules and provides affinity to hydrocarbon-chain of fatty acids of phospholipids. These polar groups are protonated at physiological pH which means that the compounds are likely to be positively charged in the physiological environment and preferentially interact with anionic membrane lipids. Once inserted in plasma membrane the orientation and localization of DMAP groups promotes their rapid diffusion towards the cytosol. It is expected that once in cytosol they move into mitochondria driven by electrophoretic movement.

Data obtained in the present study demonstrate that **OK 198** (Figure 7), **OK 208** (Figure 8) and **DK 43** (Figure 9) triterpenoid derivatives inhibit cell proliferation especially in cancer cell lines for the concentrations and time points in study. It is a very interesting result since that the main goal of anticancer drugs is to kill more effectively cancer cells, sparing normal cells [53] although based in this technique we cannot conclude if they undergo cell death induction or cell cycle arrest.

According to the previously study that reported mitochondrial structure and function alterations in the presence of these triterpenoid derivatives in melanoma cells [60] and in order to better understand the results from the proliferation assay, we further used epifluorescence microscopy to investigate *in situ* mitochondrial effects and nuclear apoptotic alterations. The fluorescent probe Mitotracker Red was used not only to detect alterations in mitochondrial membrane polarization but also to have an idea of the mitochondrial network morphology. **OK 236** does not present any visible effect on cell growth, mitochondrial morphology or polarization for the cell lines, concentrations and time points chosen (Figure 10; Figure 12 to 17). By its turn, **OK 221** proved to be a strong cell proliferation inhibitor for all the cell lines and a potent disruptor of mitochondrial function (Figure 11; Figure 12 to 17). Surprisingly, for both time points tested (48 and 96h) the selected concentration of **OK 198** (0.5 µg/ml)

induced a mild mitochondrial fragmentation in normal fibroblasts and a profound mitochondrial fragmentation and depolarization for cancer cell lines (Figure 12 to 17). Mitochondrial fission can be associated with apoptosis induction [1, 31] and oxidative stress [74] which may suggest that **OK 198** may cause oxidative stress, which should be verified in further studies. Despite the concentrations chosen for **OK 208** (2 µg/ml) and **DK 43** (1 µg/ml) did not present a markedly effect on cell growth inhibition in untransformed cell line when compared with cancer cell lines (Figure 8 and 9, respectively), the same induced a striking fragmentation and depolarization of the mitochondrial network (Figure 12 to 17). Some apoptotic-like nuclei are visible after 96 hours of time exposure in MCF-7 (Figure 17) which supports the idea that triterpenoid derivatives could exert their toxic activity by promoting apoptosis. In general, these results are in agreement with the previous study [60].The results for 48 and 96 hours were not dissimilar probably because only the most resistant adherent cells are visible.

Since the previous study [60] demonstrated that mitochondria structure and function is compromised in melanoma cell lines after incubation with the triterpenoid derivatives presence, we investigated whether the test compounds exert direct effects on isolated rat hepatic mitochondria in order to gain more mechanistical insights. Although normal hepatic and cancer cell mitochondria present some structural and functional differences [75], we believe that sufficient similarities exist to justify using isolated hepatic mitochondria as models to gain insight into the interactions of tested compounds with mitochondria. Isolated mitochondrial fractions have been used as a biological model by pharmaceutical companies as a sensitive and reliable biosensor for drug-induced toxicity [2].

The results show that **OK 198** appears to have an effect in ATP synthase Fo subunit as suggested by the decrease in ADP/O ratio (Figure 23) and the tendency to mitochondrial depolarization increase (Table 1). **OK 236**, **DK 43** e **OK 208** did not present any alteration in respiratory parameters, with the exception of the RCR decrease for **OK 236** and **DK 43** (Figure 23). The results also suggest that some of the compounds studied may present a mix of effects between inhibition of the respiratory chain and uncoupling effect, which is observed, for example by the immediate depolarization observed upon addition of the compounds to the mitochondrial suspension. Further assays will be performed to clarify which is the case for each compound. One example of multiple levels of mitochondrial toxicity is

OK 221, which appears to have a protonophoretic/ uncoupler effect and at the same time appearing to inhibit the phosphorylative system (Figure 23), seen as a tendency to decrease the depolarization induced by ADP (Table 5). Both effects contribute to the increase in phosphorylative lag phase and a drop in the ADP/O.

Two distinct experiments (mitochondrial swelling and $\Delta\psi_m$ fluctuations) demonstrate that increasing concentrations of **OK 198**, **OK 208** and **OK 221** induce the mitochondrial permeability transition pore (Figure 29). The results obtained for **OK 198** and **OK 208** are very interesting for the present study since both induce the mitochondrial permeability transition pore at concentrations that do not present a marked toxic effect on mitochondrial metabolism (Figure 23). The maintenance of the mitochondrial metabolism integrity is extremely important because apoptosis is an ATP-dependent process [4]. With these results, it is predictable that **OK 198** and **OK 208** DMAP derivatives may induce cell death through a mitochondrial permeability transition pore-related mechanism. It has been previously demonstrated that this phenomenon is considered very important, not only in the crossroad between apoptosis and necrosis, but also in organ dysfunction during different pathologies [76]. As observed in cell experiments and mitochondrial oxygen consumption, **OK 236** did not present any effect in MPTP for the concentrations and time points tested (Figure 29), which is again convincing evidence that mitochondrial effects underlie the toxicity of these agents. Unlike what was expected from results in cells, **DK 43** did not shown toxicity on any mitochondrial respiratory parameter studied (Figure 23) or caused induction of the mitochondrial permeability transition pore (Figure 29) for the concentrations tested which leads us the idea that **DK 43** may exert its activity on cancer cells independently of direct mitochondrial effects.

We can also speculate that DMAP triterpenoid derivatives activity depends on DMAP group position. Although **OK 198** and **DK 43** are theoretically similar (Figure 6) since both compounds have the same number of positive charges at physiological pH and differ only in the DMAP position groups, their effect are notably distinct. As expected for **OK 236**, the lower affinity to lipid membrane and low positive net charge was reflected by the absence of activity in models tested which confirm that compounds must have an amphiphilic character and be positively charged to exert their biological activity on organelles with the highest negative potential inside, such as mitochondria.

Conclusion

CHAPTER 5

In general, the present work corroborate the idea that DMAP triterpenoid derivatives are promising in cancer therapy since that some of the compounds present somewhat more selectivity towards cancer cells than normal cells. Moreover, mitochondrial experiments demonstrate that these agents can directly induce MPT pore in a concentration that did not interfere with normal mitochondrial metabolism, suggesting this may be a very valid mechanism that explains their toxicity. Further assays are clearly needed to explore the mechanisms of mitochondrial toxicity of the test compounds in more detail, since the borderline between a desired pharmacological effect (i.e. disruption of mitochondrial function in cancer cells) and a toxic side-effect (mitochondrial toxicity in non-target organs) is very thin indeed.

References

CHAPTER 6

1. Jeong, S.Y. and D.W. Seol, *The role of mitochondria in apoptosis.* BMB Rep, 2008. **41**(1): p. 11-22.
2. Pereira, C.V., et al., *Investigating drug-induced mitochondrial toxicity: a biosensor to increase drug safety?* Curr Drug Saf, 2009. **4**(1): p. 34-54.
3. Van Houten, B., V. Woshner, and J.H. Santos, *Role of mitochondrial DNA in toxic responses to oxidative stress.* DNA Repair (Amst), 2006. **5**(2): p. 145-52.
4. Wang, C. and R.J. Youle, *The role of mitochondria in apoptosis*.* Annu Rev Genet, 2009. **43**: p. 95-118.
5. Jezek, P. and L. Plecita-Hlavata, *Mitochondrial reticulum network dynamics in relation to oxidative stress, redox regulation, and hypoxia.* Int J Biochem Cell Biol, 2009. **41**(10): p. 1790-804.
6. Scatena, R., et al., *The role of mitochondria in pharmacotoxicology: a reevaluation of an old, newly emerging topic.* Am J Physiol Cell Physiol, 2007. **293**(1): p. C12-21.
7. Zick, M., R. Rabl, and A.S. Reichert, *Cristae formation-linking ultrastructure and function of mitochondria.* Biochim Biophys Acta, 2009. **1793**(1): p. 5-19.
8. Detmer, S.A. and D.C. Chan, *Functions and dysfunctions of mitochondrial dynamics.* Nat Rev Mol Cell Biol, 2007. **8**(11): p. 870-9.
9. Grandemange, S., S. Herzig, and J.C. Martinou, *Mitochondrial dynamics and cancer.* Semin Cancer Biol, 2009. **19**(1): p. 50-6.
10. Anesti, V. and L. Scorrano, *The relationship between mitochondrial shape and function and the cytoskeleton.* Biochim Biophys Acta, 2006. **1757**(5-6): p. 692-9.
11. Soubannier, V. and H.M. McBride, *Positioning mitochondrial plasticity within cellular signaling cascades.* Biochim Biophys Acta, 2009. **1793**(1): p. 154-70.
12. Wallace, D.C. and W. Fan, *Energetics, epigenetics, mitochondrial genetics.* Mitochondrion, 2010. **10**(1): p. 12-31.

13. Twig, G., et al., *Tagging and tracking individual networks within a complex mitochondrial web with photoactivatable GFP.* Am J Physiol Cell Physiol, 2006. **291**(1): p. C176-84.
14. Shadel, G.S., *Mitochondrial DNA, aconitase 'wraps' it up.* Trends Biochem Sci, 2005. **30**(6): p. 294-6.
15. Vockley, J. and D.A. Whiteman, *Defects of mitochondrial beta-oxidation: a growing group of disorders.* Neuromuscul Disord, 2002. **12**(3): p. 235-46.
16. Gilkerson, R.W., J.M. Selker, and R.A. Capaldi, *The cristal membrane of mitochondria is the principal site of oxidative phosphorylation.* FEBS Lett, 2003. **546**(2-3): p. 355-8.
17. Hebert, S.L., I.R. Lanza, and K.S. Nair, *Mitochondrial DNA alterations and reduced mitochondrial function in aging.* Mech Ageing Dev, 2010. **131**(7-8): p. 451-62.
18. Perez-Matute, P., M.A. Zulet, and J.A. Martinez, *Reactive species and diabetes: counteracting oxidative stress to improve health.* Curr Opin Pharmacol, 2009. **9**(6): p. 771-9.
19. Balaban, R.S., S. Nemoto, and T. Finkel, *Mitochondria, oxidants, and aging.* Cell, 2005. **120**(4): p. 483-95.
20. Hanahan, D. and R.A. Weinberg, *The hallmarks of cancer.* Cell, 2000. **100**(1): p. 57-70.
21. Galluzzi, L., et al., *Mitochondrial gateways to cancer.* Mol Aspects Med, 2010. **31**(1): p. 1-20.
22. Kroemer, G. and J. Pouyssegur, *Tumor cell metabolism: cancer's Achilles' heel.* Cancer Cell, 2008. **13**(6): p. 472-82.
23. Morselli, E., et al., *Anti- and pro-tumor functions of autophagy.* Biochim Biophys Acta, 2009. **1793**(9): p. 1524-32.
24. Grad, J.M., E. Cepero, and L.H. Boise, *Mitochondria as targets for established and novel anti-cancer agents.* Drug Resist Updat, 2001. **4**(2): p. 85-91.
25. Biasutto, L., et al., *Mitochondrially targeted anti-cancer agents.* Mitochondrion, 2010. **10**(6): p. 670-81.
26. Fulda, S., L. Galluzzi, and G. Kroemer, *Targeting mitochondria for cancer therapy.* Nat Rev Drug Discov, 2010. **9**(6): p. 447-64.
27. D'Souza, G.G., et al., *Approaches for targeting mitochondria in cancer therapy.* Biochim Biophys Acta, 2010.
28. Martin, D.N. and E.H. Baehrecke, *Caspases function in autophagic programmed cell death in Drosophila.* Development, 2004. **131**(2): p. 275-84.
29. Kerr, J.F., A.H. Wyllie, and A.R. Currie, *Apoptosis: a basic biological phenomenon with wide-ranging implications in tissue kinetics.* Br J Cancer, 1972. **26**(4): p. 239-57.
30. Sheridan, C. and S.J. Martin, *Mitochondrial fission/fusion dynamics and apoptosis.* Mitochondrion, 2010. **10**(6): p. 640-8.
31. Arnoult, D., *Mitochondrial fragmentation in apoptosis.* Trends Cell Biol, 2007. **17**(1): p. 6-12.
32. Jourdain, A. and J.C. Martinou, *Mitochondrial outer-membrane permeabilization and remodelling in apoptosis.* Int J Biochem Cell Biol, 2009. **41**(10): p. 1884-9.
33. Tait, S.W. and D.R. Green, *Mitochondria and cell death: outer membrane permeabilization and beyond.* Nat Rev Mol Cell Biol, 2010. **11**(9): p. 621-32.
34. Ulivieri, C., *Cell death: insights into the ultrastructure of mitochondria.* Tissue Cell, 2010. **42**(6): p. 339-47.
35. Saelens, X., et al., *Toxic proteins released from mitochondria in cell death.* Oncogene, 2004. **23**(16): p. 2861-74.

36. Grimm, S. and D. Brdiczka, *The permeability transition pore in cell death.* Apoptosis, 2007. **12**(5): p. 841-55.
37. Martinou, J.C. and D.R. Green, *Breaking the mitochondrial barrier.* Nat Rev Mol Cell Biol, 2001. **2**(1): p. 63-7.
38. Zamzami, N., N. Larochette, and G. Kroemer, *Mitochondrial permeability transition in apoptosis and necrosis.* Cell Death Differ, 2005. **12 Suppl 2**: p. 1478-80.
39. Wong, W.W. and H. Puthalakath, *Bcl-2 family proteins: the sentinels of the mitochondrial apoptosis pathway.* IUBMB Life, 2008. **60**(6): p. 390-7.
40. Leung, A.W. and A.P. Halestrap, *Recent progress in elucidating the molecular mechanism of the mitochondrial permeability transition pore.* Biochim Biophys Acta, 2008. **1777**(7-8): p. 946-52.
41. Baines, C.P., *The mitochondrial permeability transition pore and ischemia-reperfusion injury.* Basic Res Cardiol, 2009. **104**(2): p. 181-8.
42. Baines, C.P., *The molecular composition of the mitochondrial permeability transition pore.* J Mol Cell Cardiol, 2009. **46**(6): p. 850-7.
43. Solaini, G., et al., *Hypoxia and mitochondrial oxidative metabolism.* Biochim Biophys Acta, 2010. **1797**(6-7): p. 1171-7.
44. Kroemer, G., *Mitochondria in cancer.* Oncogene, 2006. **25**(34): p. 4630-2.
45. Chandra, D. and K.K. Singh, *Genetic insights into OXPHOS defect and its role in cancer.* Biochim Biophys Acta, 2010.
46. Yu, M., et al., *Reduced mitochondrial DNA copy number is correlated with tumor progression and prognosis in Chinese breast cancer patients.* IUBMB Life, 2007. **59**(7): p. 450-7.
47. Lin, Y.W., et al., *Roles of glutamates and metal ions in a rationally designed nitric oxide reductase based on myoglobin.* Proc Natl Acad Sci U S A, 2010. **107**(19): p. 8581-6.
48. Hung, W.Y., et al., *Somatic mutations in mitochondrial genome and their potential roles in the progression of human gastric cancer.* Biochim Biophys Acta, 2010. **1800**(3): p. 264-70.
49. Fantin, V.R. and P. Leder, *Mitochondriotoxic compounds for cancer therapy.* Oncogene, 2006. **25**(34): p. 4787-97.
50. Wang, F., M.A. Ogasawara, and P. Huang, *Small mitochondria-targeting molecules as anti-cancer agents.* Mol Aspects Med, 2010. **31**(1): p. 75-92.
51. Modica-Napolitano, J.S. and J.R. Aprille, *Delocalized lipophilic cations selectively target the mitochondria of carcinoma cells.* Adv Drug Deliv Rev, 2001. **49**(1-2): p. 63-70.
52. Ralph, S.J. and J. Neuzil, *Mitochondria as targets for cancer therapy.* Mol Nutr Food Res, 2009. **53**(1): p. 9-28.
53. Nguyen, D.M. and M. Hussain, *The role of the mitochondria in mediating cytotoxicity of anti-cancer therapies.* J Bioenerg Biomembr, 2007. **39**(1): p. 13-21.
54. Costantini, P., et al., *Mitochondrion as a novel target of anticancer chemotherapy.* J Natl Cancer Inst, 2000. **92**(13): p. 1042-53.
55. Gershenzon, J. and N. Dudareva, *The function of terpene natural products in the natural world.* Nat Chem Biol, 2007. **3**(7): p. 408-14.
56. Krasutsky, P.A., *Birch bark research and development.* Nat Prod Rep, 2006. **23**(6): p. 919-42.
57. Alakurtti, S., et al., *Pharmacological properties of the ubiquitous natural product betulin.* Eur J Pharm Sci, 2006. **29**(1): p. 1-13.

58. Lin, Y.C., et al., *Analgesic and anti-inflammatory activities of Torenia concolor Lindley var. formosana Yamazaki and betulin in mice.* Am J Chin Med, 2009. **37**(1): p. 97-111.
59. Fulda, S. and G. Kroemer, *Targeting mitochondrial apoptosis by betulinic acid in human cancers.* Drug Discov Today, 2009. **14**(17-18): p. 885-90.
60. Holy, J., et al., *Dimethylaminopyridine derivatives of lupane triterpenoids are potent disruptors of mitochondrial structure and function.* Bioorg Med Chem, 2010. **18**(16): p. 6080-8.
61. Selzer, E., et al., *Effects of betulinic acid alone and in combination with irradiation in human melanoma cells.* J Invest Dermatol, 2000. **114**(5): p. 935-40.
62. Fulda, S., *Betulinic acid: a natural product with anticancer activity.* Mol Nutr Food Res, 2009. **53**(1): p. 140-6.
63. Papazisis, K.T., et al., *Optimization of the sulforhodamine B colorimetric assay.* J Immunol Methods, 1997. **208**(2): p. 151-8.
64. Skehan, P., et al., *New colorimetric cytotoxicity assay for anticancer-drug screening.* J Natl Cancer Inst, 1990. **82**(13): p. 1107-12.
65. Cardoso, C.M., et al., *Mechanisms of the deleterious effects of tamoxifen on mitochondrial respiration rate and phosphorylation efficiency.* Toxicol Appl Pharmacol, 2001. **176**(3): p. 145-52.
66. Gornall, A.G., C.J. Bardawill, and M.M. David, *Determination of serum proteins by means of the biuret reaction.* J Biol Chem, 1949. **177**(2): p. 751-66.
67. Moreira, P.I., et al., *Mitochondria from distinct tissues are differently affected by 17beta-estradiol and tamoxifen.* J Steroid Biochem Mol Biol, 2011. **123**(1-2): p. 8-16.
68. Chance, B., G.R. Williams, and G. Hollunger, *Inhibition of electron and energy transfer in mitochondria. III. Spectroscopic and respiratory effects of uncoupling agents.* J Biol Chem, 1963. **238**: p. 439-44.
69. Chance, B. and G.R. Williams, *The respiratory chain and oxidative phosphorylation.* Adv Enzymol Relat Subj Biochem, 1956. **17**: p. 65-134.
70. Oliveira, P.J., et al., *Inhibitory effect of carvedilol in the high-conductance state of the mitochondrial permeability transition pore.* Eur J Pharmacol, 2001. **412**(3): p. 231-7.
71. Kamo, N., et al., *Membrane potential of mitochondria measured with an electrode sensitive to tetraphenyl phosphonium and relationship between proton electrochemical potential and phosphorylation potential in steady state.* J Membr Biol, 1979. **49**(2): p. 105-21.
72. Broekemeier, K.M., M.E. Dempsey, and D.R. Pfeiffer, *Cyclosporin A is a potent inhibitor of the inner membrane permeability transition in liver mitochondria.* J Biol Chem, 1989. **264**(14): p. 7826-30.
73. Oliveira, P.J., et al., *Carvedilol inhibits the mitochondrial permeability transition by an antioxidant mechanism.* Cardiovasc Toxicol, 2004. **4**(1): p. 11-20.
74. Wu, S., et al., *Mitochondrial oxidative stress causes mitochondrial fragmentation via differential modulation of mitochondrial fission-fusion proteins.* FEBS J, 2011. **278**(6): p. 941-54.
75. Gogvadze, V., B. Zhivotovsky, and S. Orrenius, *The Warburg effect and mitochondrial stability in cancer cells.* Mol Aspects Med, 2010. **31**(1): p. 60-74.
76. Rasola, A. and P. Bernardi, *The mitochondrial permeability transition pore and its involvement in cell death and in disease pathogenesis.* Apoptosis, 2007. **12**(5): p. 815-33.